reactions

MDPI

Review

Dual Roles of Coke in Fresh and Modified HY Zeolite Catalyzed Aromatic Alkylation: Mechanisms, Structural Transformations, and Catalyst Regeneration

Alhumam A. Al-Shammari [1], Bashir Y. Al-Zaidi [1] and Ali Al-Shathr [2,*]

[1] Department of Chemical Process Engineering, College of Chemical Engineering, University of Technology-Iraq, Baghdad 10066, Iraq; che.22.16@grad.uotechnology.edu.iq (A.A.A.-S.); bashir.y.sherhan@uotechnology.edu.iq (B.Y.A.-Z.)

[2] Department of Petroleum Refining and Gas Technology Engineering, College of Chemical Engineering, University of Technology-Iraq, Baghdad 10066, Iraq

* Correspondence: ali.r.mohammedjawad@uotechnology.edu.iq

Abstract

Linear alkylbenzene (LAB) is the main raw material used to make biodegradable detergents, and its production process is based on aromatic alkylation. HY zeolites that have undergone controlled dealumination and desilication have led industrial standards amongst solid acid catalysts because of their controllable acidity and hierarchical pore structure. Coke formation in such systems can assume a dual role, which is dependent on its condition. Though the over-deposition is known to cause deactivation by blocking the micropores, Bronsted acid-site masking, and diffusion collapse, the low-level deposition could also be done to increase the monoalkylate selectivity by the pore mouth catalysis, steric modulation, and selective suppression of secondary alkylation pathways. The critical review is done on the structural-kinetic interaction that determines the coke evolution in HY-based catalysts. In order to moderate the acid-site density and enhance hydrothermal stability, dealumination (Si/Al optimization of about 2.5 to 30–100) occurs, but to reduce deep-pore coke formation, desilication (interconnected mesopores) is created. The bimodal porosity and regulated acidity are found to be synergistic, as hierarchical HY zeolites produced through successive cycles of steam and alkaline treatments not only show LAB selectivity in excess of 90% but also exhibit much longer catalyst lifetimes. Quantitative research on the beneficial coke regime revealed that it was composed of about 36 wt% hydrogen-rich species, which were localized at the pore mouths, hence enhancing monoalkylation selectivity by 15–40%. Beyond a critical transition window (e.g., 8–12 wt.%), coke formation to condensed polyaromatic and graphitic products leads to fast deactivated coke formation, which is due to percolation limits and transport-controlled kinetics. More advanced techniques of characterization of the coke, e.g., temperature-programmed oxidation (TPO), ^{27}Al MAAS NMR, and UV-Raman spectroscopy, indicate how the coke is changed to highly structured graphitic deposits of high oxidation activation energy. Activity recovery of 85–98% is obtained in regeneration processes, including controlled oxidative calcination, microwave-based and plasma-based processes, and thermal management protocols, and it would be determined by the chemistry of the coke, its spatial distribution, and the regeneration protocols. This paper has developed a mechanistic coke control system by cross-tuning the acidity and development of an effective pore network, which led to a sustainable aromatic alkylation reaction with minimal activity loss, high selectivity, and long life.

Check for updates

Academic Editor: Simonetta Tuti

Received: 7 February 2026
Revised: 27 February 2026
Accepted: 3 March 2026
Published: 11 March 2026

Copyright: © 2026 by the authors. Licensee MDPI, Basel, Switzerland. This article is an open access article distributed under the terms and conditions of the Creative Commons Attribution (CC BY) license.

Keywords: aromatic alkylation; HY zeolite; coke formation; dealumination; desilication; pore mouth catalysis; linear alkylbenzene; catalyst regeneration

1. Introduction

Aromatic alkylation is very vital in the petrochemical industry, especially in the synthesis of LAB, which is a major intermediate in the manufacture of biodegradable surfactants [1,2]. The LAB market is expected to be worth billions, with a compound annual growth rate (CAGR) of 3.8%, and it is set to grow to $14.2 billion by 2030 as the Asia-Pacific region advances towards its own environmentally friendly detergents needs and grows its share of the market, which currently comprises about 60% of the overall usage [3–5]. LAB is the precursor to the most commonly used surfactant in household and industrial cleaning products, linear alkylbenzene sulfonate (LABS), which is a paradigm shift to biodegradable alternatives to branched-chain alkylbenzenes, which are environmentally persistent [6–9]. Conventional aromatic alkylation methods use homogeneous catalysts, including hydrofluoric acid (HF) and aluminum chloride ($AlCl_3$), which present a serious environmental, safety, and operational problem [10,11]. These liquid-acid systems produce dangerous waste, need corrosion-proof infrastructure and pose threats of disastrous accidents. As a result, the design of heterogeneous catalysts using zeolites has become strategic, and the benefits associated with this approach are simplicity of separation, reusability, less corrosivity, and absence of liquid-acid risks (see Figure 1) [12–19].



Figure 1. Conceptual framework of market, catalytic, and environmental drivers in aromatic alkylation.

The Y-type zeolites based on faujasite (FAU) topology are one of the most appealing zeolitic materials, as they feature three-dimensional pore structures, large supercages (12.4 Å diameter), abundant Brønsted acidity, and the capability to receive both aromatic compounds and olefin reactants [20–22]. Dealumination and desilication are the best after-synthesis reagents [23,24]. Dealumination is a process that selectively removes the atom framework aluminum in the form of steaming, acid leaching or chemical extraction to purify the Si/Al ratio to 30–100, reducing the density of acid sites, enhancing hydrothermal stability, and forming secondary porosity [25,26]. In desilication, alkaline treatment is used to selectively remove silicon atoms to produce hierarchical mesoporosity, which increases diffusion and decreases the mass transfer restrictions and the importance of internal active sites [27,28]. In spite of such developments, the process of coke formation continues to be the major deactivation process that restricts the life and productivity of industrial catalysts [23].

Coke carbonaceous deposits that have been formed during the processes of olefin oligomerization, alkylation-dealkylation, hydrogen transfer, and cyclization-dehydrogenation reactions, which accumulate on catalyst surfaces and in the pore structures, increasingly cover up the active sites and active diffusion pathways [29–31]. Notably, the responses of coke are highly different between dealuminated HY zeolites and desilicated hierarchies [2,23], which requires sophisticated characterization methods (TPO, NMR, UV-Raman spectroscopy) to reveal structure–activity–deactivation correlations [32–35]. According to recent mechanistic research, a paradigm shift has occurred where coke is no longer harmful but can be dualistic with regard to quantity, chemical composition and spatial distribution [23,36]. The accumulation of soft aliphatic coke at pore mouths in a controlled manner can be useful in increasing shape selectivity, and reducing polyalkylation, but the too high deposition of the graphitic coke in the micropores leads to permanent deactivation [23]. These two aspects have significant implications for catalyst design and regeneration techniques.

This paper provides an in-depth analysis of coke manufacture in the case of dealuminated and desilicated HY zeolite-catalyzed aromatic alkylation. It is aimed to: (1) systematically study the influence of dealumination and desilication on zeolite structure, acidity and porosity; (2) understand the mechanisms, pathways of evolution, and space distributions of coke formation; (3) be critical about the dual role of coke as a deactivating agent and characterization of selectivity; (4) assess advanced characterization methods of coke analysis; and (5) to evaluate regeneration options of sustainable industrial alkylation processes. The proposed study will enable the next generation of hierarchical zeolites to be developed in terms of greater coke tolerance, more regenerable and greater catalytic performance through the combination of reaction engineering, zeolite chemistry and materials characterization.

2. Zeolite Catalysts: Structure and Properties

2.1. HY Zeolite Framework Characteristics

HY zeolite, which has the FAU (faujasite) topology, is one of the most studied and commercially used catalysts in the aromatic alkylation processes [20,21]. It has a crystalline structure made up of a three-dimensional network of huge supercages (12.4 internal diameter) linked together by 12-membered ring (12-MR) windows and effective pore apertures of about 7.4 Å [37–41]. Such a clear microporous structure permits the efficient diffusion of aromatic molecules, including benzene, toluene, and xylene, but provides steric hindrance, essentially preventing the formation of bulky branched isomers in favor of linear (n-alkyl) products [21,42–44]. This large cavity volume and size-discriminating pore entrance combination has made HY zeolite the catalyst of choice in the industrial synthesis of LAB and other shape-selective aromatic reactions [45].

The framework Si/Al ratio is the main determinant of the catalytic activity of HY zeolites and directly regulates the Brønsted acid site density, acid strength, hydrothermal stability, and deactivation resistance [46,47]. Si/Al ratios of 1.5–3.0 in parent HY materials indicate a high level of framework aluminum and, therefore, a high level of acidity (Brønsted). As shown in Figure 2, each tetrahedrally connected complex structure aluminum atom ($[AlO_4]^-$) provides a negative charge that is countered by a proton to create a Brønsted acid site (Si-OH-Al). This forms a nearly stoichiometric association between the concentration of aluminum and an acid site, a correlation that has been comprehensively confirmed by ^{27}Al MAS NMR, NH_3-TPD, and pyridine adsorption data [48,49].

The controlled dealumination, which is attained through steaming (500–800 °C in controlled humidity), acid leaching with dilute mineral acids, or chelation with complexing agents like EDTA, gradually raises the Si/Al ratio to an intermediate level (usually 30–100), which is known to be the most favorable level to be used in aromatic alkyla-

tion [50–52]. The key impact of dealumination is the regulated decrease and rearrangement of Brønsted acid sites, which is accompanied by partial formation of extra-framework aluminum (EFAl) species that bring in secondary Lewis acidity and focal defects of the framework [52–54]. Notably, although extreme dealumination may produce defect-related vacuoles or restricted secondary porosity, compositional and acidic modulation, as opposed to deliberate mesopore formation, is the most common. On the contrary, desilication-based treatments are also more effective at producing large and well-controlled mesoporosity, and silicon is selectively removed to form hierarchical pore structures (see Section 3.1). This difference is important to ensure that the relationships between structure and functions are not misinterpreted in modified HY catalysts.

Dealuminated HY zeolites have an optimum balance between the density of the acid and structural stability in the intermediate Si/Al range (30–100). Low-Si/Al (Si/Al 10) materials are too acidic and thus favor polyalkylation and coke formation; highly siliceous material (Si/Al 150) has a low acid density that creates low catalytic activity [55,56]. The experiments indicate benzene conversions and selectivity of LAB in this optimized compositional regime up to more than 90% under industrially relevant conditions [12,57]. It is more active because it has moderate acid-site density, desirable spatial positions of active sites in supercages, steric control at 12-MR windows, which prevents secondary alkylation, and higher resistance to hydrothermal decay and formation of coke [58–60]. This advantage has resulted in the industrial standards of LAB production becoming the best dealuminated HY zeolites, offering a good tradeoff between activity, selectivity, stability, and regenerability.

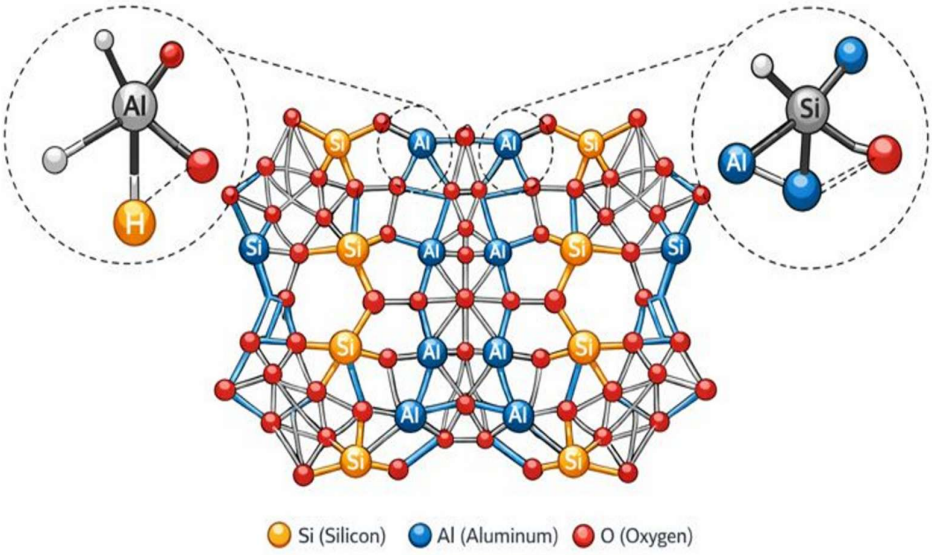


Figure 2. The Si-O-Al bonds in the FAU (HY zeolite) framework were illustrated structurally, reproduced from [61].

The hierarchical pore structure of HY zeolite, which consists of intrinsic micropores formed in the crystalline aluminosilicate structure and secondary mesopores formed in the process of dealumination, plays an important role in catalyzing alkylation of large aromatic molecules [28,62–64]. Mesoporosity has a huge effect on the region of mass transport in the fact that it increases diffusion pathways as well as decreases diffusion resistance [65]. This bilateral pore network not only hastens the reaction of the reactions, but it also promotes the outflow of products in addition to reducing the build-up of heavy intermediates that are precursors of coke [23]. As a result, hierarchical structures have high catalytic activity and extend catalyst lifetimes by minimizing the deactivation caused by diffusion [66]. Hierarchical zeolites have transport characteristics that are important in ensuring high throughput and stability in operation in commercial alkylation [67].

2.2. Comparative Analysis of Zeolite Types

Although HY zeolite is predominant in the industrial aromatic alkylation, knowledge of other zeolite topologies gives valuable background to its greater performance, see Figure 3. The structure of Beta zeolite (BEA) consists of a complex three-dimensional pore network composed of two interconnected channel systems: straight 12-membered ring (12-MR) channels (6.6 × 6.7 Å) and sinusoidal channels (5.6 × 5.6 Å) [68–70]. This dual-channel structure is used to ease the passage of reactants and intermediates through the zeolite structure. BEA zeolite has a range of Si/Al ratios 10–100, which gives variable acidity and good stability of the framework [71,72]. Such compositional ratios produce moderate to high Brønsted acid site densities that are correct enough to experience an alkylation reaction. The blend of acidity and hydrothermal stability of BEA zeolite ensures the material is very suitable in the industrial processes that need to be done in high temperatures with the presence of water [73]. Recent reports show that the addition of cerium (Ce) to BEA zeolite through the one-pot hydrothermal synthesis method has had a tremendous boost on the catalytic activity [74–76]. BEA zeolite modified with Ce has enhanced activity and stability in the alkylation of benzene with dodecyl alcohol, which is commercially significant. The improved performance is attributed to the synergistic interactions between cerium species and Brønsted acid sites, where cerium species facilitate electron transfer and the formation of reactive intermediates, while Brønsted acid sites promote electrophilic aromatic substitution [77,78]. Ce-immobilized BEA zeolite has a greater conversion rate, better selectivity and a longer lifespan than other BEA systems, which is commercially feasible in industrial alkylation processes [79].

The ZSM-5 zeolite (MFI) structure has a special structure of straight channels (5.3 × 5.6 Å) and intersecting sinusoidal ones (5.1 × 5.5 Å) at a right angle [80–82]. The dual-channel system generates a shape-selective three-dimensional network that regulates the transport of molecules and the stabilization of transition states in the zeolite structure. Although this architecture gives an outstanding control over product distribution, the pore apertures are relatively small and severely sterically restrict the applicability of ZSM-5 to alkylation reactions with large-molecule aromatics [54,83]. Therefore, ZSM-5 can only be used with smaller aromatic substrates. ZSM-5 has a characteristic physicochemical property, which means a high Si/Al ratio that is usually 20 to 200 [84–86]. This compositional range offers medium and yet controlled Brønsted acidity as well as excellent hydrothermal and thermal stability. The stability measured acidity and controlled pore geometry allow ZSM-5 to do well in selective catalytic tasks where strict shape selectivity, resistance to deactivation, and performance under harsh conditions are needed [84,87]. The above properties render ZSM-5 essential in reactions like methanol-to-hydrocarbons (MTH), methanol-to-olefins (MTO), and selective hydrocarbon upgrading, whereby the discrimination of a particular molecule and the ability of the structure are of prime significance [88].

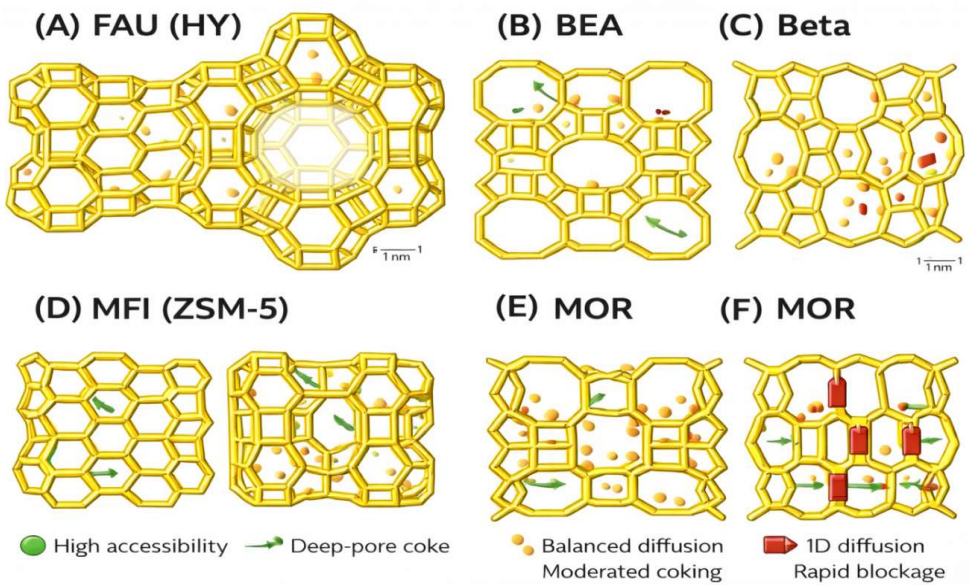


Figure 3. Zeolite framework topology and diffusion pathways in aromatic alkylation. (**A**) FAU (HY) zeolite, (**B**) BEA zeolite, (**C**) Beta zeolite framework demonstrating medium pore accessibility and diffusion pathways, (**D**) MFI (ZSM-5) zeolite, (**E**) MOR zeolite displaying one-dimensional channels where diffusion limitations may occur and (**F**) MOR structure showing severe pore blockage as a result of coke formation leading to rapid catalyst deactivation, reproduced from [89].

Zeolite topology is critical to the selection of topology to use in industrial applications based on the measurements of reactant/product molecular dimensions, shape selectivity that is required, and process severity [90]. Zeolites differ greatly in pore structure, acidity distribution, diffusion and structural stability, as shown in Table 1. HY zeolite provides an ideal ratio of physicochemical characteristics in the case of aromatic alkylation [91]. Having a hierarchical pore structure, which consists of intrinsic micropores and secondary mesopores that are created by controlled dealumination, it offers channels of the right size to take on large aromatic compounds yet permits efficient intracrystalline transport and product desorption [92]. Architecture improves mass transfer, minimizes diffusion barriers, and coke formation, and increases the catalyst lifetime. The effectiveness and selectivity of electrophilic aromatic substitution reactions in HY zeolite is very high due to the strategic location of Brønsted and Lewis acid sites [93,94]. Together with the hydrothermal and thermal stability of the framework, the combination facilitates the maintenance of the HY zeolite to sustain harsh industrial treatments and high temperatures without structural deterioration. All these benefits make HY zeolite the most dependable and industrially favored catalyst to be used in aromatic alkylation reactions [2,20,21].

Table 1. Structural, acidic, and catalytic characteristics of representative zeolites used in aromatic alkylation (compiled from [95] and the related literature under reported reaction conditions).

Parameter	HY (FAU)	HY-DA	BEA	BEA–Ce	ZSM-5	MOR
Framework topology	FAU	FAU	BEA	BEA	MFI	MOR
Pore system	3D, 12-MR	3D + mesopores	3D, 12-MR	3D, 12-MR	3D, 10-MR	1D, 12-MR
Pore size (Å)	7.4	7.4	6.6–6.7	6.6–6.7	5.1–5.6	6.5–7.0
Si/Al ratio	2.5–6	30–100	10–100	15–80	20–200	10–20
Acidity (mmol NH_3 g^{-1})	1.8–2.5	0.4–0.8	0.6–1.4	0.7–1.2	0.3–0.8	1.0–1.8
Mesoporosity	Low	High	Low	Low	Very low	Low
Typical temperature (°C)	150–250	150–250	160–240	160–240	180–260	170–250

Table 1. *Cont.*

Parameter	HY (FAU)	HY-DA	BEA	BEA–Ce	ZSM-5	MOR
WHSV (h^{-1})	1–3	1–3	1–2	1–2	1–3	1–2
Benzene/olefin molar ratio	5–10	5–10	4–8	4–8	3–6	4–8
Pressure (MPa)	1–3	1–3	1–3	1–3	1–3	1–3
Benzene conversion (%)	75–85	90–98	82–92	88–95	65–78	70–82
LAB selectivity (%)	70–80	88–96	82–90	86–93	60–75	75–85
Catalyst lifetime (h)	8–12	24–48	12–18	18–28	6–10	10–15
Coke tolerance	Low	High	Moderate	High	Low	Moderate
Main application	Heavy alkylation	Industrial LAB	LAB production	Advanced LAB	Light aromatics	Linear alkylation
Relative cost	1.0×	1.3–1.5×	1.4–1.6×	2.0–2.5×	1.2–1.4×	1.1–1.3×

3. Structural Modifications: Dealumination and Desilication

3.1. Dealumination Processes and Mechanisms

The most widely used post-synthesis modification strategy to tune the structure of HY zeolites to be used in aromatic alkylation is dealumination [51,96]. Dealumination makes it easy to control the density of acid sites, hydrothermal stability, and pore structure, reducing coke formation and improving catalyst life. As illustration in Table 2, the main delamination pathways are included in the steam treatment, acid leaching, extraction by chelation using EDTA, and treatment by ammonium hexafluorosilicate (AHFS) [12,23,25,53,97]. Steam dealumination is still the industrial technique of choice, as it is simple and scalable. When HY zeolites are exposed to water vapor at high temperatures (500–800 °C), hydrolytic cleavage of Al-O-Si bonds occurs, causing the extraction of framework aluminum and the migration of some species of aluminum [25,98]. The rate of dealumination is strongly temperature-sensitive; little dealumination happens below 200 °C, dealumination is initiated by controlled aluminum migration at 300–400 °C, and poorly controlled dealumination at temperatures higher than 500–400 °C. Although EFAL species generate Lewis acid sites that promote alkylation reactions, excessive EFAL deposition can block zeolite pores. Therefore, acid washing is often applied after EFAL formation to remove excess species and create secondary mesoporosity [96,99,100].

Moderate temperatures (60–100 °C) of acid leaching with mineral acids (HCl or HNO_3, 0.1–6 M) selectively remove the EFAL species but do not substantially destroy the zeolite framework [51,96,101]. This method offers excellent crystalline retention, yet produces minimal mesoporosity, resulting in only limited enhancement of mass transport. Another method that is highly selective, using multidentate complexation to remove aluminum under the conditions of controlled pH and temperature (pH 4–7, 80–100 °C), is EDTA chelation [101–103]. Although this method offers high preservation of structure and the dealuminations are under control, the high cost of reagents and the complexity of the operations limit the application of this method to only laboratory-scale use. The AHFS treatment has been found to be a promising new advanced method that can form HY zeolites with extremely high Si/Al ratios (>50) and effective EFAL removal [53,97]. Aluminum-silicon reinsertion into the aluminum framework vacancies with the aid of fluoride results in well-defined mesoporosity and optimal acidity. Nonetheless, related environmental issues associated with the waste of fluoride are currently restricting mass industrial applications.

Table 2. Comparison of dealumination methods for HY zeolite modification in aromatic alkylation.

Parameter	Steam	Acid Leaching	EDTA	AHFS
Typical conditions	500–800 °C, H_2O	0.1–6 M acid, 60–100 °C	0.1–0.5 M, pH 4–7	0.1–1.0 M, 60–95 °C
Si/Al ratio	15–50	10–40	20–80	30–100
Framework Al removal (%)	40–70	30–60	50–80	60–85
EFAL formation	High	Moderate	Low	Very low
Mesoporosity ($cm^3\ g^{-1}$)	0.10–0.18	0.05–0.12	0.12–0.20	0.15–0.25
Crystallinity retention (%)	75–90	85–95	90–98	80–92
Benzene conversion (%)	90–96	85–92	88–94	92–98
LAB selectivity (%)	88–94	84–90	86–93	90–96
Catalyst lifetime (h)	24–36	18–28	20–32	30–48
Scalability	Excellent	Excellent	Good	Moderate
Cost (relative)	Low	Low	High	Moderate
Industrial status	Widely applied	Common	Research-scale	Emerging
Key references	[25,59,98,104–106]	[51,96,101]	[101,103,107]	[53,97]

Experimental results indicate that temperature significantly influences the dealumination process, while the zeolite framework type determines its thermal stability and response to temperature. Zeolite structures are condensed and dealumination is reduced at 200 °C [108,109]. The majority of aluminum atoms are structural; the structure does not lose much metal. The change of framework aluminum species is ordered at 300 °C [105,106,110]. The heat totally eliminates the atoms of aluminum in the structure. The migration of the aluminum of tetrahedral coordination to an extra-framework causes the chemical composition and geometry of the zeolite to be altered as shown in Figure 4. This temperature-sensitive transformation needs stringent testing of the thermal conditions for essential adjustment [111].



Figure 4. Sequential structural modification of ZSM-5 zeolite via desilication and dealumination, reproduced from [112].

The catalyst can be altered by extra-framework aluminum species defects during dealumination [96,99,113]. Mesopores could be produced by acid rinsing or Lewis acid sites. The residual acid site strength and concentration are affected by dealumination. Dealumination increases high-quality, rare acid sites [100]. Steam treatment does not remove aluminum as well as chemical dealumination using complexing agents such as ethylenediaminetetraacetic acid [101,102]. These compounds will tend to bind to aluminum atoms to extract them easily and cause minimal structural damage, complexing solution pH, temperature, and concentration to optimize dealumination [103].

3.2. Desilication Processes and Structural Modifications

Desilication is one post-synthetic step where framework silicon is selectively removed to produce hierarchical zeolite crystallization, which is a combination of microporous shape selectivity and mesoporous diffusion catalysis [114–117]. Desilication facilitates access to secondary mesopore networks, which could previously not be alkylated with large aromatic substrates, and increases the accessibility, activity, and catalyst lifetime [27,28]. Ordinary desilication agents include sodium hydroxide (NaOH), potassium hydroxide (KOH) and organic bases, e.g., tetra-propylammonium hydroxide (TPAOH), of which the selection determines the silicon extraction intensity, silicon extraction location and silicon extraction selectivity [117,118]. The key parameters that are worth regulating include the concentration of alkali, temperature, treatment time and, above all, the Si/Al ratio that makes the frameworks resistant to attack by alkali [119–121]. When the conditions are favorable, silicon-rich zeolites (Si/Al > 15) are selectively desilicated at the crystal surfaces yet with minimal loss of internal structure order, allowing one to regulate the production of uniform mesopores without appreciably losing crystallinity [20,122–125]. It is suggested that reintroduction of post-desilication of aluminum in mesopore walls can regenerate the available Br3nsted acidity in the newly formed porosity that further enhances catalytic performance [54,114,126]. However, when over-alkaline or over-treated for a long time, hyper desilication takes place, leading to framework dissolution, amorphization and loss of performance [28,127]. Such risks will be minimized through the use of pore-directing agents, e.g., tetrabutylammonium hydroxide (TBAOH), to spatially concentrate on silicon extraction and preserve long-range order by selectively inhibiting alkaline attack [128–130].

Figure 5 schematically shows that interconnected mesopores are formed during controlled alkaline desilication, but the microporous structure remains, which is used in shape selectivity [131–134]. The resultant bimodal pore structure synergistically integrates molecular separations with improved mass transportation, an element that is of great importance in aromatic alkylation of large molecules, which are severely diffusion-limited in pure microporous zeolites [28,114,135]. Through rational parameter control, typically with reinsertion of aluminum, ordered hierarchical zeolites with optimized acidity and diffusion pathways can be designed [136–139]. Table 3 gives a comparison of desilication routes that can easily be applied to aromatic alkylation.

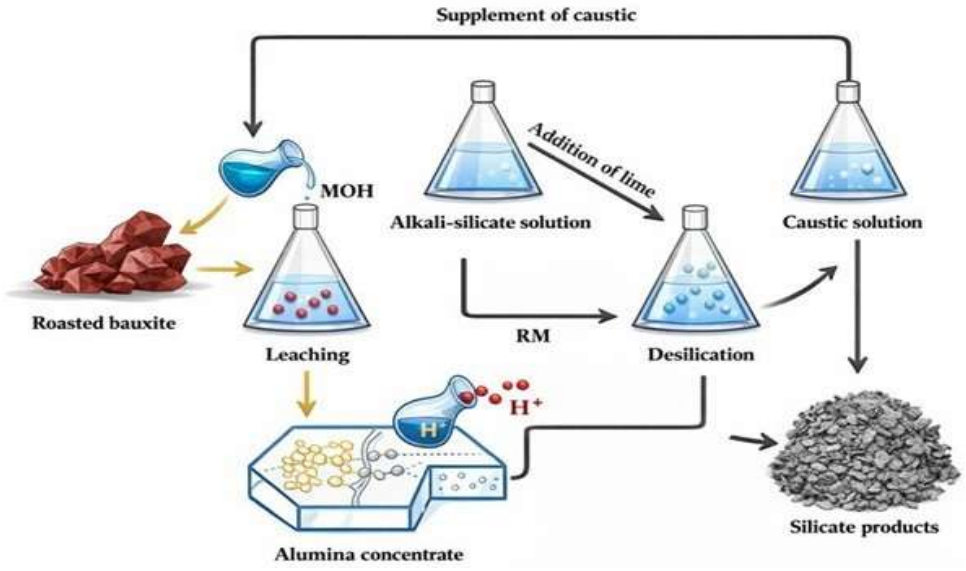


Figure 5. Schematic illustration of the desilication process modeled on alkaline leaching of roasted bauxite, reproduced from [131].

Table 3. Desilication strategies for hierarchical HY zeolites in aromatic alkylation.

Method	NaOH	KOH	TPAOH	Sequential (NaOH → Steam)
Typical conditions	0.1–0.5 M, 60–85 °C	0.1–0.4 M, 70–90 °C	0.05–0.2 M, 80–95 °C	0.2 M NaOH + 600 °C steam
Si/Al ratio	8–15	10–18	12–20	25–45
Mesopore volume ($cm^3\ g^{-1}$)	0.15–0.25	0.12–0.22	0.10–0.18	0.18–0.30
Crystallinity (%)	70–85	75–88	80–92	75–90
Brønsted sites (mmol g^{-1})	0.8–1.2	0.9–1.3	1.0–1.4	0.5–0.9
Conversion (%)	88–94	90–95	85–92	93–99
LAB selectivity (%)	85–92	87–94	83–90	91–98
Lifetime (h)	28–42	32–48	24–38	40–60
Coke (wt.%)	5.8–7.5	5.2–6.8	6.5–8.2	3.8–5.5
Scalability/Cost	Excellent/Low	Excellent/Low	Moderate/High	Good/Moderate
Industrial status	Widely used	Common	Limited	Emerging
Key refs	[114–118,140]	[117–121]	[128–130]	[28,105,141,142]

3.3. Combined Dealumination–Desilication Strategies

Sequential dealumination–desilication is a complicated framework-engineering methodology of forming hierarchical zeolites with enhanced structural, textural and catalytic capability than isolated post-synthesis additions [140,143,144]. The sequence of treatments is conclusive: dealumination proceeds to desilication, which is always more homogeneous in mesoporosity, retains its crystallinity, and has higher catalytic activity than the reverse sequence [118]. This is due to the mechanistic interaction between the defect formation of the framework and selective silicon mining. The first step of dealumination forms structures vacations and silanol sites or defects, which serve as favorable nucleation sites in the second step of alkaline desilication [145]. These locations facilitate the creation of spatially regulated silicon elimination and generate interlinked mesopores of optimal size and connectivity [90,146]. In this regard, dealumination is a successful way of preparing the zeolite structure to undergo hierarchical pore formation.

Steam pretreatment is also linked to the improvement of sequential modification protocols [28,105,141]. Through thermal treatment, other framework defects are introduced, hydrolytic susceptibility is enhanced, and any residual organics or water that might cause the inhibition of further chemical treatments are removed [90,109]. Steam-dealumination-desilication routes thus produce clear bimodal pore structures, where conserved micropores guarantee molecular selection, and newly created mesopores, to allow quick diffusion and product desorption [147–150]. These hierarchical architectures offer transformational benefits to aromatic alkylation of large molecules [28,151,152]. The purely microporous zeolites pose a strong diffusion constraint on long-chain olefins and alkylated products, and hence low conversion and rapid deactivation by pore blockage. Decoupling selectivity and transport operations in hierarchical zeolites addresses such limitations: micropores are selective to linear monoalkylated, and mesopores are highly permeable to diffusion and coke formation [54,98,153,154].

Sequential modification also allows a specific control of structural evolution of the parent HY zeolite to the ultimate hierarchical catalyst, as schematically shown in Figure 6 [155–160]. Framework Al-O-Si bonds are controlled to be dealuminated forming silanol nests which direct further alkaline desilication (see Figure 6) [156,157]. The secondary mesopores thus formed are linked to the remaining microporous network to form a synergistic micro-mesoporous architecture that gives rise to molecular selectivity and increased mass transport [159]. More complex designs in advanced designs, silanol nests

formed in the dealumination step, can be further functionalized with metal species (e.g., Ti added in Cp_2TiCl_2), creating extra Lewis acidic centers and expanding the catalytic range beyond Brønsted acids [155,158]. These hierarchical systems of zeolites are multifunctional with low diffusion barriers, increased access to operational sites and improved resistance to deactivation in troublesome reactions of alkylation [159,160].

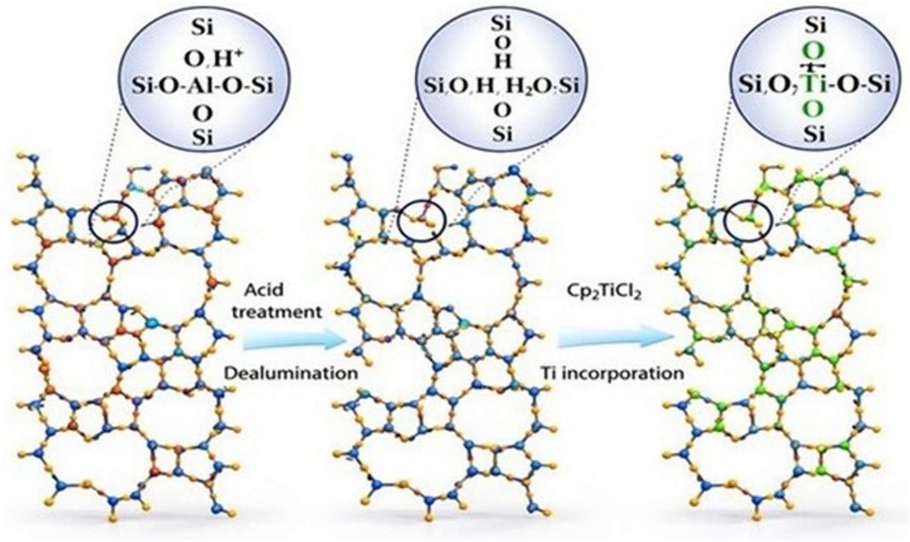


Figure 6. Schematic representation of structural evolution in HY zeolite during dealumination and desilication processes, reproduced from [155].

4. Dual Role of Coke: Detrimental Versus Functional Effects

The formation of coke during the aromatic alkylation on HY zeolites has long been considered a major reason for catalyst deactivation expressed through the blockage of the micropores, masking of the Br-acid sites, and extreme restriction of intracrystalline diffusion [23,114,161]. Nevertheless, its effect is not necessarily harmful, but it highly depends on the coke loading, molecular structure, and spatial distribution of the zeolite structure. Figure 7 shows that the light aliphatic or weakly aromatic species with the relatively high H/C ratios that predominantly form during low coke coverages (usually around 350,500 wt.% H in FAU-type HY zeolites) are present at low coverages and are localized at the pore mouths and exterior surfaces [23,36,162,163]. The secondary alkylation and bulky transition states are suppressed, and the internal micropore is retained, which increases the selectivity of the monoalkylate product, with pore mouth catalysis being a geometric modulator when a partial pore mouth constriction is used in this regime [91,164]. Experimental investigations on FAU-, BEA-, and MOR-type zeolites support the fact that this controlled coke deposition enhances selectivity without causing considerable diffusional breakdown [164,165]. As time-on-stream or conditions of more adverse reactions increase, successive dehydrogenation and condensation produce polyaromatic and graphitic species of coke with low H/C ratios and higher structural rigidity [166–169]. These condensed species move into intracrystalline micropores and fill up more and more, covering Bronsted acid sites and causing nonlinear decreases in effective diffusivity and catalytic activity. When coke loading toward a critical transition zone, the coke loading is usually on the order of 8–12 wt.%; in the case of standard HY catalysts, micropore occupancy reaches a percolation threshold at which there are no interconnected diffusion pathways anymore and rapid deactivation ensues [23,170].

Notably, the frequently used and commonly cited 10 wt.% value is not universal in nature, as it is dictated by the inherent volume and connectivity of FAU structures; in other words, the functional-to-detrimental transition is a percolation phenomenon of structure

and is not merely a concentration value. Sequential dealumination-desilication can make hierarchical HY zeolites that improve mass transport, slow the coke deposition in the deep pores, and push the deactivation point to higher coke loadings, thereby stabilizing functional coke species and increasing catalyst life [28,63,96,171]. As a result, coke is not only to be considered as a catalyst poison but rather as a dynamic structural modifier, the formation of which can be controlled to be optimally exploited with regard to selectivity, stability, and overall efficiency in industrial aromatic alkylation.

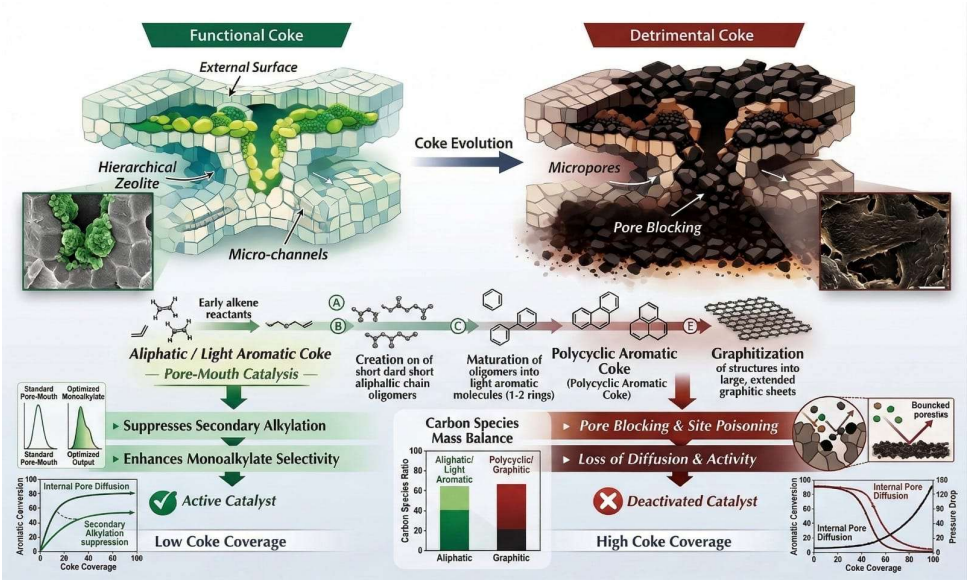


Figure 7. Dual role of coke in HY zeolite-catalyzed aromatic alkylation: from pore mouth selectivity to micropore deactivation.

5. Previous Studies

The zeolites are considered to be the best catalysts in aromatic alkylation due to their adjustment to acidity, thermal stability, and shape-selective microporous structures [152]. Specifically, HY zeolite (FAU) containing 12-membered-ring supercages easily accepts benzene, toluene, as well as higher aromatics in the industrial environment [114,161]. However, coke formation is still the predominant deactivation mechanism, which gradually blocks Brønsted acid sites, impedes intracrystalline diffusion and reduces catalyst life when operating under extended high temperature conditions [172]. In an effort to overcome this deactivation caused by coke, extensive research has been done on framework engineering. The most successful single modification has been found to be dealumination, which enhances the Si/Al ratio, reduces undue acidity and improves hydrothermal stability [103]. This strategy is supported by desilication, which selectively removes silicon in alkaline media to add mesoporosity without affecting the inherent shape selectivity of the microporous framework [12]. The pioneering studies of Verboekend and Perez-Ramirez have shown that with the use of controlled alkalinity, temperature and pore-directing agents, diffusion is greatly enhanced because mesopores are formed in the presence of crystallinity without loss of crystallinity [152,173].

Subsequently, narrower sequential dealumination-desilication methods have been justified, with hierarchical micro-mesoporous HY zeolites having better catalytic properties [12]. Multi-scale pore structure hybrid steam-alkaline treatments decouple the operations of selectivity and transport: micropores retain molecular selectivity, mesopores are high-accessibility active sites and achieve rapid product removal [143]. Li et al. have shown a 140% lifetime increase in the catalysts in difficult hydrocarbon conversions because of the shortened diffusion routes and equal Brønsted/Lewis acidity distribution [63]. These

hierarchical structures suppress condensation reactions, leading to refractory polyaromatic coke [174]. The design of rational catalysts is founded on a mechanistic theory of the way in which coke is generated. The coke formation on acid zeolites is a sequential process of olefin oligomerization, cyclization, aromatization and condensation to polycyclic aromatics, predominantly on Brønsted sites [166,167]. Coke has always been viewed as an evil substance but lately it has been established that it has dual importance. Al-Shathr et al. demonstrated that the selectivity of monoalkylated could be increased during controlled deposition of coke through the mouths of the micropores due to geometric inhibition of over-alkylation, commonly denoted as pore mouth selectivity, that occurred in both beta and mordenite zeolites [23]. These findings lead to the opposite of the traditional paradigm and suggest that it is strategic coke management that would generate the optimal performance of catalysts and not the complete inhibition of it.

There are still important knowledge gaps, even with the massive progress made. The existing literature (as summarized in Table 4) indicates that (i) quantitative correlations of hierarchical pore architecture with topology of coke deposition are necessary, (ii) the switch between the beneficial and detrimental coke has to be explained, (iii) and that strong structure–activity relationships under industrially relevant conditions, and (iv) the spatial distributions of coke between micro-, meso-, and mesopores have to be solved [11,173,175,176]. By filling these gaps, it will be possible to rationally design next-generation HY-based catalysts with superior coke tolerance, regenerability and long-term stability to support sustainable processes of aromatic alkylation.

Table 4. Selected studies on modified HY zeolites and coke formation in aromatic alkylation.

Authors (Year)	Zeolite/ Modification	Reaction	Si/Al	Coke (wt.%)	k (h^{-1})	Conv. (%)	LAB Sel. (%)	Lifetime (h)	Key Outcome	Ref.
Zhang et al. (2024)	Beta–Ce	Benzene + C_{12}	18	5.8	0.024	93	91	32–45	Metal acid synergy	[74]
Al-Sultani et al. (2024)	HY	Toluene + C_8	38	6.5	0.028	91	89	28–38	Kinetic validation	[21]
Al-Shathr et al. (2023)	Beta and mordenite controlled coke	Toluene + C_7	25	3.8	0.015	95	92	40–55	Pore mouth catalysis	[23]
Li et al. (2017)	HY, steam dealumination and desilication	Heavy aromatics	45	5.2	0.022	94	–	36–48	140% lifetime increase	[63]
Verboekend et al. (2013)	HY, dealumination and desilication	Hydrocarbons	48	4.8	0.019	96	–	42–58	Lowest deactivation rate	[171]
Verboekend and Pérez-Ramírez (2011)	HY, desilication	Model alkylation	12	7.5	0.038	90	86	22–30	Mesopores improved diffusion	[114]
Horňáček et al. (2010)	HY, dealumination	Benzene + C_{12}	42	6.8	0.032	92	88	24–32	High regenerability	[177]
Da et al. (2001)	HY, steam dealumination	Toluene + C_{12}	35	8.2	0.045	89	85	18–24	35% coke reduction verses parent	[91]

6. Aromatic Alkylation Reaction Mechanisms

6.1. Eley-Rideal Mechanism and Reaction Pathways

Aromatic alkylation with zeolite catalysts uses a proton-mediated electrophilic substitution reaction that is not mechanistically related to classical homogeneous Friedel-Crafts chemistry (see Figure 8) [12,178]. In conventional systems using $AlCl_3$, the coordination reaction of the alkylating agent with the Lewis acid yields a relatively free carbocation in the bulk liquid phase, which then reacts with the aromatic ring without steric constraints. No pore blockage enables the free movement of carbocations, but also facilitates uncontrolled polyalkylation and side reactions [21].

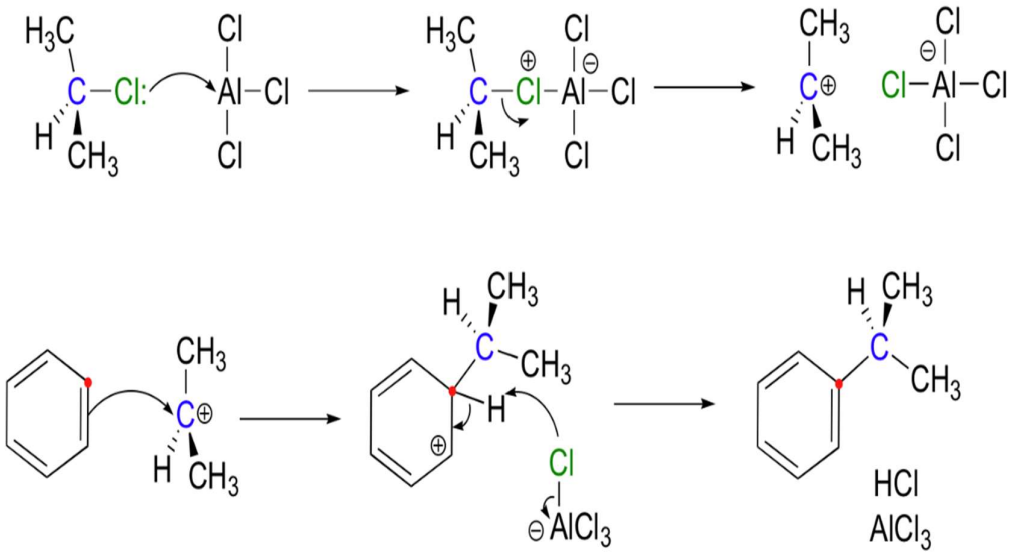


Figure 8. The classical homogeneous Friedel-Crafts alkylation mechanism, with $AlCl_3$ as a Lewis acid catalyst, demonstrates the formation of carbocation in bulk-phase and electrophilic aromatic substitution [179].

In the alkylation of zeolites in the opposite direction, the Brønsted acid sites (Si-OH-Al) (protonated olefin) are prototransformed in a closed micropore; the olefin is protonated by zeolite channels to form a carbenium ion anchored to the zeolite structure [21,178,180]. This is the protonation step, more generally known as the rate-limiting step, which is governed by the strength of the acid, proton affinity, framework polarization, and local electrostatic stabilization. Unlike homogeneous systems, reactive intermediates in zeolites are spatially confined, and their reactivity is strongly influenced by the pore topology and steric constraints.

An Eley-Rideal (ER) mechanism is frequent in the reaction, where the protonated olefin (adsorbed species) reacts with an aromatic molecule entering the liquid phase [181]. It is not a definite but a conditional description. When such a situation as increased aromatic adsorption intensity or improved surface coverage occurs, a Langmuir-Hinshelwood (LH)-type of mechanism, i.e., the momentary co-adsorption of the reactants within the pore network, can become dominant [182]. As such, the ER and LH pathways cannot be considered mutually exclusive but instead as competing or complementary pathways, the relative abundance of which is determined by adsorption energies, concentrations of reactants, pore structure, and diffusion rates [183]. In LAB it is customary that weakly adsorbed benzene and strongly adsorbed olefin protons in large-pore FAU-type zeolites, which are actually desired in large-scale LAB production, preferentially adsorb onto ER-like surfaces, yet medium-pore or diffusion-limiting situations can also have a beneficial impact on LH contributions [12].

Figure 9 shows the electrophilic attack by the protonated carbenium ion on the surface is accompanied by the protonated carbenium ion attacking the aromatic π-system of the protonated carbenium ion to form a σ-complex (Wheland intermediate), which, although not a permanent breaking of aromaticity, occurs temporarily [21,44,181]. Aromatic structure deprotonation is later recovered and the Brønsted acid site is regenerated, which completes the catalytic process. The stability of carboxylations and regioselectivity of acids in the presence of acids are certain determinants of carboxylations' stability and regioselectivity, which ultimately determine the distribution of the product. The stability of the intermediate is highly affected by the pattern of substitution, the effect of hyperconjugation, and the affixation of the intermediate in the zeolite pore.

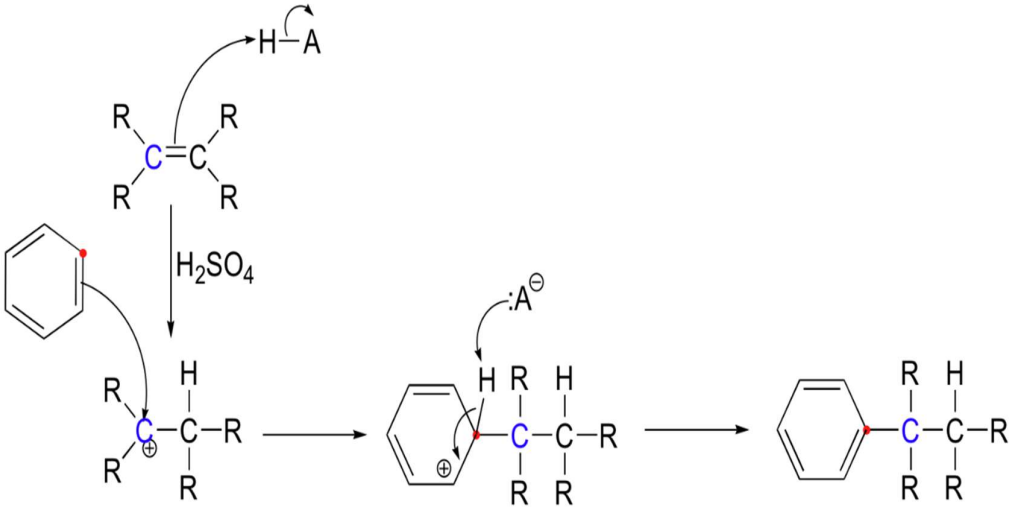


Figure 9. Proposed zeolite-mediated aromatic alkylation mechanism on Brønsted acid sites, illustrating olefin protonation, formation of a surface-stabilized carbenium ion, σ-complex generation, and regeneration of the acid site within a confined microporous environment [179].

Notably, mass transport within the zeolite structure is important for controlling the expression of mechanistic properties. The effect of intracrystalline diffusion constraints on adsorption equilibria, effective concentrations of reactants at active sites, and transition-state stabilization [12,21]. As the coke gradually fills pore mouths and intracrystalline micropores, adsorption of geometries and steric constraints are altered, potentially shifting the relative contribution of ER-type surface interactions versus diffusion-limited LH-type interactions. Accordingly, aromatic alkylation on the HY zeolites must not be considered as one or the other mechanistic pathway but as a confinement-controlled, proton-mediated, electrophilic substitution network, wherein the strength of the acid, the topology of the pore, the resistance to diffusion, and the coke evolution are all-determining catalytic performance, selectivity, and coke evolution.

6.2. Selectivity Control and Product Distribution

The aromatic alkylation of numerous different compounds with zeolite catalysts results in mono- or di-alkylated products based on the reaction and catalyst conditions [162]. Mono-alkylation is carried out under moderate conditions of reaction, such as low temperature and concentration of olefins, due to less electrophilic substitution of aromatic rings. The combination of higher temperatures and increased olefin concentration facilitates di-alkylation since the number of reactive carbenium ions that can be substituted will increase [184]. Larger di-alkylated molecules are synthesized and diffused more selectively by steric constraints, whereas mono-alkylation is elevated when the aperture of the pore is small [170]. HY zeolite strikes a balance between molecular accessibility and shape

selectivity of the catalyst to maximise mass-transport rates and steric control [21,165]. Dealumination improves electrophilic aromatic substitution on its hierarchical pore structure. Recent studies indicate that dealuminated HY zeolites can be expected to have a long industrial catalytic lifetime and LAB selectivity of more than 90% [177]. Molar ratios of aromatic to olefin (5:1 to 10:1) are known to enhance mono-alkylation selectivity and have no effect on the rates of the reaction in the high-purity LAB [162].

The efficiency, selectivity, and stability of aromatic alkylation reactions between hydrocarbons rely on temperature compared to acidic zeolite catalysts [2,12]. The temperature range is 90–250 °C, which is the best range of temperatures, balancing between catalyst stability and reaction kinetics. The elevation of temperature produces and reacts to carbocation intermediates required in electrophilic aromatic substitution, accelerating the reaction. Olefin oligomerization, cracking and heavy polyalkylated species can occur with high temperatures [169,185]. Byproducts directly modify the deposition of coke on the zeolites on the pore networks and block the active sites, diffusion pathways, and catalysts. The rate of alkylation versus temperature is Arrhenius, as with the acid-catalyzed reaction pathways [21]. Because of the low energy barrier of olefin protonation and carbocation generation, the rate-limiting step of most alkylation systems, an appropriate temperature control in the temperature interval of 40–80 kJ/mol has also been observed to preserve the energy barrier in reactions. The catalyst has to be shielded because of the lower temperature, the reaction has to be selective, and the production of coke has to be reduced [186].

7. Coke Formation: Mechanisms and Characterization

The actual process of coke formation in aromatic alkylation on HY zeolite can be considered mechanistically, as Figure 10 demonstrates, right-to-left, starting with the final graphitic lamellae of carbon and progressing to the sources of the carbon atoms within their molecules [187]. At the extreme right-hand of the sequence with low H/C ratios, extended polyaromatic stacking and adsorption on the interior walls of the pore or external catalyst surfaces, very condensed graphitic domains are observed [23]. These reserves are the thermodynamic limit of converting hydrocarbons into acidic conditions. These are very structured domains with lower hydrogen content, making it hard to deprotonate by oxidation. This organization drastically limits access to micropores, exposes Brønsted acid locations and influences transport.

As these graphitic structures develop to the left, they are formed out of progressively condensed polycyclic aromatic hydrocarbons (PAHs) [168,188,189]. PAHs are formed by repeated electrophilic substitution, dehydrogenation, and intermolecular cross-linking reactions that take place under high temperature and high Brønsted acidity. Planarization, π-π stacking, and stabilization of aromatic intermediates are facilitated by confinement effects in the supercages of FAU-type HY zeolites, and this process enhances the rate at which the intermediates of these interfaces undergo transformation into larger, less hydrogenated carbon frameworks. At this point, there is a reduction in molecular mobility, growth in diffusional resistance, and the catalyst starts to shift away from reaction-controlled performance to transport-limited deactivation.

Further left in the series, PAHs are synthesized based on monocyclic and oligocyclic aromatic intermediates, which are synthesized by cyclization of unsaturated hydrocarbon oligomers [57,170]. These intermediates are a derived product of surface-bound carbenium ions that are due to the protonation of olefins at Brønsted acid sites. Aromatic species of increasing stability are produced by oligomerization, followed by an intramolecular ring closing and aromatization. This chemistry is not completely decoupled from selective alkylation in optimal conditions, but high temperature, high olefin partial pressure, or high density of acid sites switches the reaction network to condensation-dominated reactions.

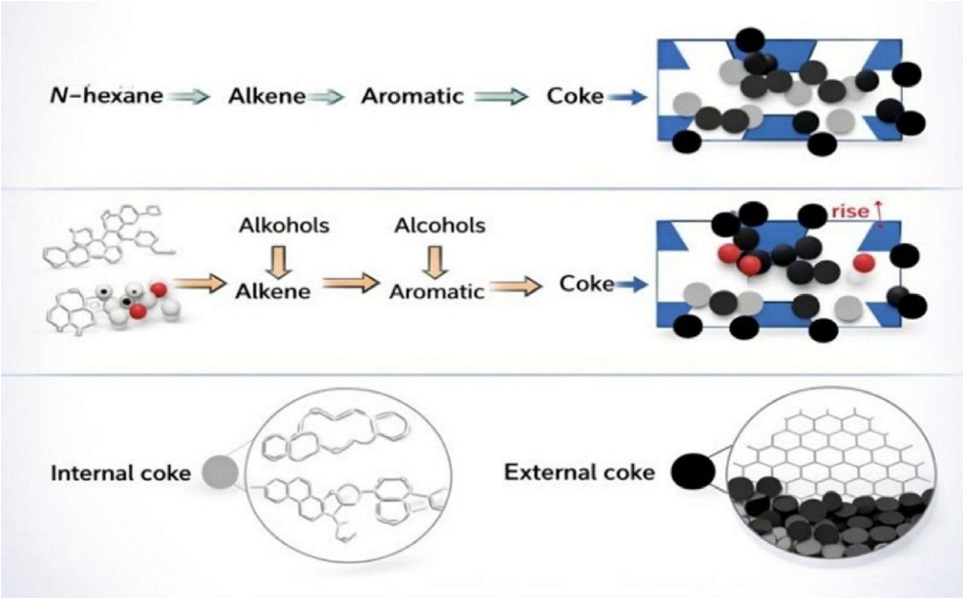


Figure 10. Reverse mechanistic interpretation of coke evolution in HY zeolite during aromatic alkylation, illustrating the transformation from graphitic coke (**right**) to polyaromatic intermediates and light hydrocarbon precursors (**left**) within a confined microporous framework. Adapted from [187].

The protonation and activation of light hydrocarbons (olefins, paraffins, alkyl intermediates) in the zeolite micropore system occur at the leftmost point of origin of the scheme. This initial step controls the desirable electrophilic aromatic substitution, and it is linked with moderate intrinsic activation energies (usually 4080 kJ mol^{-1}), which represent the barrier to the energy necessary for olefin protonation and the formation of 3-complex [162]. These intermediates undergo productive alkylation preferentially with control of the reaction conditions. Nevertheless, stronger thermal or acidic conditions trigger the identical reactive carbocation species to act as a site of nucleation in oligomer growth and later evolution of coke.

Kinetically, the right-to-left reconstruction is able to account for this apparent variability of the experimentally determined activation energies as time-on-stream increased. To begin with, the activation energies that are observed are predominantly chemical barriers that are inherent [190]. As polyaromatic intermediates accumulate and the number of micropores filled increase, the resistance of mass transfer becomes more significant, and the apparent activation energy measured by an experiment is the product of the intrinsic reaction and diffusion rate-limiting factors. Lastly, in high coke loads, the system is transport-controlled, and the nonlinear tendency in catalytic behavior is observed, which does away with the previously incompatible kinetic interpretations [31].

In general, the coke formation process must not be regarded as a discrete side reaction but rather as a thermodynamically preferred endpoint of a continuum of acid-catalyzed hydrocarbon reactions, the course of which is controlled by temperature, acidity, confinement effects, and residence time.

7.1. Coke Types and Characterization

Aromatic alkylation of coke can take place over zeolitic catalysts, and it is possible to classify coke based on its chemical composition, spatial location and thermal stability, which is highly dependent on the performance and regenerability of the catalysts (see Table 5) [166]. In gentle circumstances, the aliphatic coke, which is made of lightly unsaturated hydrocarbons, is initially formed and it is eliminated with a lot of ease during regeneration, and it usually burns at low temperatures (300–400 °C) owing to its high level

of hydrogen and low level of condensation [191,192]. This coke transforms into aromatic coke made of polyaromatic hydrocarbons of higher thermal stability as the severity of the reaction increases and more extreme oxidation temperatures (450–550 °C) are needed to remove it [23]. Additional condensation produces the most refractory coke, graphitic coke, which consists of highly fused aromatic structures, has low H/C ratios, and cannot be regenerated oxidatively, even in harsh operating conditions [193,194]. The spatial distribution of coke in the zeolite is also of crucial interest. Internal coke that is deposited inside of micropores directly obstructs Brønsted acid sites and diffusion pathways, resulting in a rapid deactivation of coke even in low concentration levels [169]. It is a coke that is usually polymeric, condensed partially and contains hydrogen [195]. Conversely, external coke builds up on crystal surfaces and pore mouths and has highly condensed polyaromatic structures with low H/C ratios and increased densities, which become increasingly limiting to mass transport and also lead to cumulative catalyst deactivation [196,197]. Taken together, coke type, the degree of condensation and the spatial location of the catalysts define the extent of catalyst deactivation, the difficulty of regenerating the catalyst and the stability of long-term operation during the zeolite-catalyzed aromatic alkylation processes [198,199].

Table 5. Characteristics of different coke types in zeolite catalysts [191].

Coke Type	Chemical Composition	H/C Ratio	Density (g/cm^3)	Formation Temperature (°C)	TPO Peak (°C)	Removal Difficulty
Aliphatic	Saturated hydrocarbons	1.8–2.0	0.8–1.0	150–250	300–400	Easy
Aromatic	Unsaturated aromatics	0.8–1.2	1.0–1.3	200–350	450–550	Moderate
Graphitic	Highly condensed PAHs	0.2–0.6	1.5–2.0	300–500	550–700	Difficult

7.2. Advanced Characterization Techniques

Advanced characterization techniques play a critical role in elucidating the chemical nature, structural evolution, and spatial distribution of coke deposits formed during aromatic alkylation over zeolitic catalysts [31]. Temperature-programmed oxidation (TPO) is one of the most widely applied methods in which spent catalysts are heated under controlled oxidative conditions while monitoring CO and CO_2 evolution [200,201]. Distinct oxidation peaks in TPO profiles provide valuable information on coke quantity, composition, and thermal stability, with hydrogen-rich, less condensed coke oxidizing at lower temperatures and highly condensed graphitic coke appearing at higher temperatures [35,202]. Furthermore, coke located within zeolite micropores typically combusts at higher temperatures due to diffusion limitations, enabling differentiation between internal and external coke deposits [203].

Solid-state nuclear magnetic resonance (NMR) spectroscopy offers complementary atomic-level insight into catalyst structure. In particular, ^{27}Al MAS NMR effectively distinguishes framework aluminum from extra-framework species formed during dealumination [204,205]. Framework Al appears as sharp resonances near 60 ppm, whereas extra-framework Al exhibits broader signals at lower chemical shifts, allowing quantitative assessment of dealumination and acid-site modification that influence coke formation and catalyst stability [113]. Ultraviolet Raman spectroscopy further enhances molecular-level characterization by selectively probing π-conjugated aromatic structures, enabling discrimination between oligomeric species, polycyclic aromatic hydrocarbons, and pre-graphitic coke domains [206]. Recent studies have demonstrated its ability to identify cyclopentadienyl cations, polyolefins, and aromatic intermediates trapped within zeolite pores during hydrocarbon conversion reactions [5,207]. Together, TPO, solid-state NMR, and UV Raman spectroscopy provide a powerful, complementary toolkit for understanding coke

chemistry, catalyst degradation, and structure–activity relationships in zeolite-catalyzed alkylation processes.

8. Catalyst Deactivation and Regeneration

8.1. Deactivation Mechanisms and Kinetic Consequences

The catalyst deactivation of aromatic alkylation on the zeolitic materials is mainly controlled by the gradual build-up of carbonaceous deposits that are formed by oligomerization, cyclization, and aromatization, as well as condensing reactions of the confined hydrocarbon intermediates [168]. Deactivation is not due to a single phenomenon but a case of three main mechanisms acting in a synergistic way, which are (i) micropore blockage, (ii) active-site masking, and (iii) framework destabilization [208].

Micropore blockage is the accumulation of carbonaceous species in channel crosses and in the inside of supercages, which progressively limits molecular diffusion to Brønsted acid sites and causes transport limitations, especially in materials with smaller pore apertures [90,209]. Active-site masking is caused by either adsorption or encapsulation of coke precursors on Brønsted and Lewis acid sites, which inhibit the protonation and curious carbonation-mediated routes to electrophilic aromatic substitution [45,210]. In long-term, high-temperature, or high-partial-pressure olefin environments, highly condensed polyaromatic coke species can impose localized mechanical and chemical demands on the framework, sometimes with incumbent partial dealumination, diminished crystallinity, or irreversible loss of acidity [32,211].

Kinetically speaking, coke is usually split into soft and firm forms. Soft coke is made of hydrogen-rich, less-condensed species, which are relatively reactive to oxidation. Hard coke, on the other hand, consists of hydrogen-deficient, highly aromatic, or graphitic domains that are more highly structured and possess much higher oxidation activation energies [60,210,212]. The oxidation barrier of graphitic coke is much greater than that of less condensed graphitic coke species, which exhibit stronger π-π interactions and greater confinement in micropores [213]. As a result, the rate of deactivation as well as the difficulty of regeneration are affected by the coke structure, the ratio of H/C, spatial distribution, and pore confinement. Such observations underline the critical role of acidity, pore structure, and diffusion channels in reducing deep-pore coke formation and slowing the shift in the behavior of the reaction in industrial aromatic alkylation to that of diffusion-limited behavior [214,215].

8.2. Regeneration Strategies and Process Optimization

The most common method of industrial zeolitic catalyst regeneration is oxidative regeneration because it is simple to perform and can be scaled [210]. Controlled oxidation of coke is normally performed in air or diluted oxygen in the range of 400–600 °C to transform carbonaceous compounds to CO_2 and H_2O to reveal once more the Brønsted and Lewis acid sites [175].

The catalytic activity recovery in conventional air calcination is normally reported to be between 85 and 90, which is a successful elimination of moderately condensed and soft coke species (see Figure 11). With optimization of regeneration regimes in terms of gradual temperature increments, progressive oxidation, controlled O_2 partial pressure, and careful observation of heat loss recovery, rates of 95–98% can be achieved. The most significant determinants of activity recovery are coke chemistry and spatial distribution: aliphatic and weakly aromatic coke deposits are easily oxidized, and even highly condensed graphitic deposits require even higher temperatures and longer exposure times, which threaten the framework dealumination, pore collapse, or partial acid sites loss [216–218].

Industrial regeneration strategies therefore employ controlled heating–cooling cycles, diluted oxidant streams, and in situ temperature feedback systems to minimize thermal runaway and structural degradation. Such approaches preserve crystallinity, maintain acid-site integrity, and enable multiple reaction–regeneration cycles without catastrophic loss of performance.

Recent developments in regeneration technology aim to enhance coke removal efficiency while reducing thermal stress. Microwave-assisted regeneration selectively heats carbonaceous deposits, promoting localized oxidation while limiting bulk lattice overheating [219,220]. Plasma-assisted regeneration generates reactive oxygen species capable of oxidizing coke at substantially lower temperatures, demonstrating particular effectiveness in removing soft and moderately condensed coke without imposing severe thermal penalties [221,222].

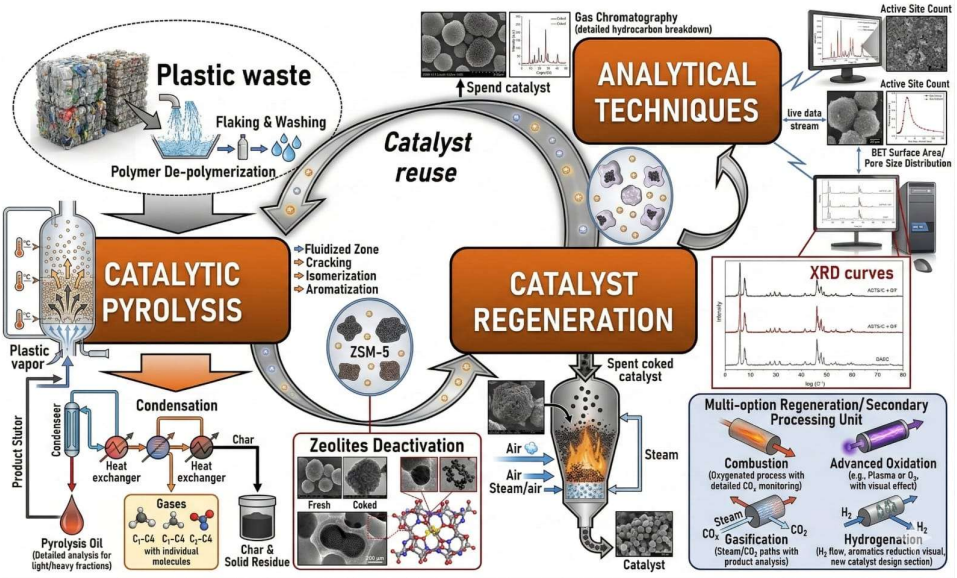


Figure 11. Schematic representation of catalyst deactivation and regeneration cycle during aromatic alkylation over HY zeolite (adapted from [45]).

Ultimately, optimal regeneration strategies must balance oxidation efficiency with structural preservation. Effective regeneration restores pore accessibility, maintains acid-site distribution, and sustains catalytic performance across repeated industrial cycles, thereby enhancing economic viability and operational stability.

9. Industrial Applications and Economic Analysis

9.1. Linear Alkylbenzene Production

Modern industrial processes of aromatic alkylation are based on modified HY zeolite catalysts, especially in the synthesis of linear alkylbenzene (LAB), a key chemical in the synthesis of biodegradable surfactants (see Figure 12) [2]. The world LAB market is projected to reach up to around 6.2 million tons in 2033, with a growth rate of 3.37 percent annually, as the demand for eco-friendly surfactants, particularly in the Asia-Pacific region, which contributes almost 60 percent of the world demand [4,223]. Dealuminated HY zeolites have good industrial performance, with a LAB selectivity of about 90%, and are highly stable and exhibit high diffusion properties, as demonstrated by the use of these catalysts in commercial solid-acid alkylation processes, including the UOP Detal process [224]. Solid zeolite catalysts have enormous benefits over the traditional liquid–acid systems, which rely on hydrofluoric acid, such as enhanced safety, minimized corrosive waste, enhanced product linearity and purity, simplified plant design, and lower operating

costs [12]. Considering the growing challenges in the environmental performance of chemicals, and the worldwide transition to sustainable chemical operations, LAB alkylation using dealuminated HY zeolites is likely to continue to be the primary focus of the global surfactant supply chain [2,225].

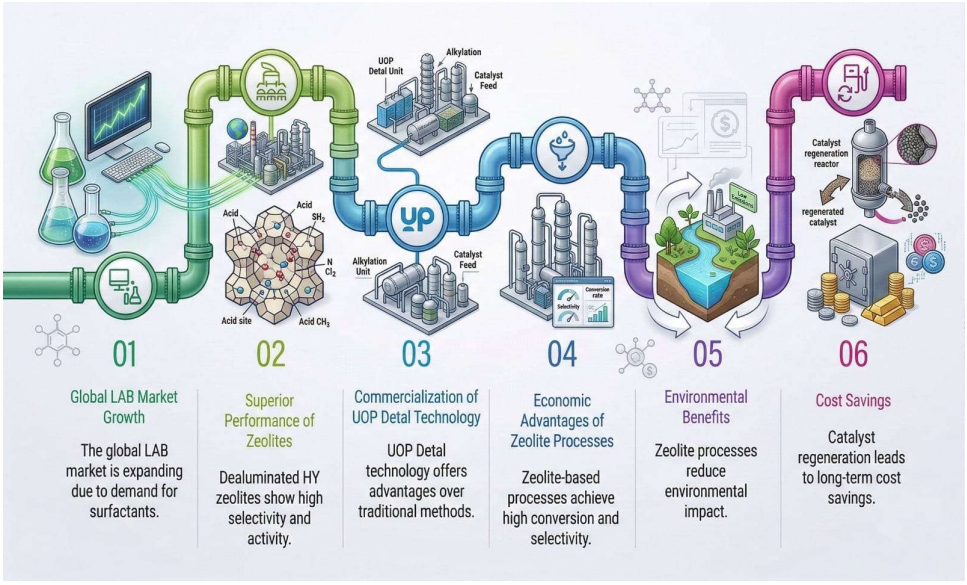


Figure 12. Key drivers and benefits of zeolite-catalyzed LAB production using UOP Detal technology.

The recent industrial case studies and techno-economic reports have clearly stated the high economic and environmental benefits of alkylation technologies based on zeolite [7]. Units of LAB production using modified HY zeolite catalysts have recorded excellent performance, with conversions of naphthalene of about 96% and mono-alkylnaphthalene selectivity of about 97.5, with comparisons showing this to be much higher than conventional liquid–acid catalytic systems [226]. The efficiencies are highly valued as they provide higher yields and throughput of the products and reduce the formation of by-products; therefore, the use of corrosive liquid acids like HF or $AlCl_3$ is eliminated, making the process of zeolite-catalyzed processes safer and easier to regulate [16,227]. The original capital cost of high-performance modified zeolite catalysts might be very expensive, but due to good regenerability and a long lifespan, the catalysts can be regenerated multiple times with minimum deactivation, therefore, saving a lot of money in the long term [190]. Together with better quality of products, less environmental liability, and a lower cost of waste-treatment, these aspects altogether emphasize the high economic rationale of using zeolite-based LAB production technologies in the contemporary industrial practice [91].

9.2. Process Integration and Optimization

In order to achieve maximum utilization of the modified HY zeolite catalysts in the industrial alkylation processes, one must pay close attention to operating conditions, reactor design and operating strategy. Close control of temperature, pressure and feed constituents is necessary to ensure the integrity of the catalyst and its activity and to avoid the early deactivation and loss of selectivity [21]. Increasingly, modern plants are using continuous reaction-regeneration systems, where catalysts in the reactor are replenished on-site, so the reactor is not shut down, which enhances operational reliability and minimizes production interruptions [166].

The process of catalyst performance is constantly checked on the basis of real-time conversion, selectivity, pressure drop, and temperature gradient measurements. In case of any early indications of deactivation, which are usually categorized by coke buildup,

catalysts are bypassed to a regeneration zone where they are processed under controlled oxidative conditions and then sent back into the reactor without interrupting the process (see Figure 13) [216]. This computerized cyclic process provides a uniform quality of products, a long catalyst life, high plant throughputs, and better overall economic output. The altered HY zeolite catalysts, through the intelligent process integration and design, permit the use of the catalysts to achieve increased efficiency, stability, and sustainability in modern aromatic alkylation reactors [12].

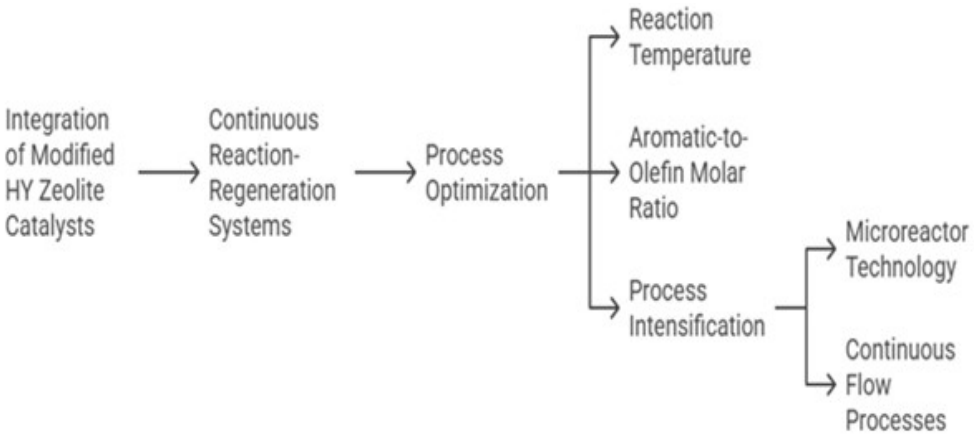


Figure 13. Key elements of process integration and optimization for zeolite-catalyzed aromatic alkylation.

Table 6 illustrates the optimization of the process in aromatic alkylation is designed to equalize the major operating variables: reaction temperature, pressure, residence time and catalyst-to-feed ratio to maximize conversion, selectivity, and catalyst life [2]. Zeolite-mediated alkylation is usually optimally catalyzed at a temperature range of 90–250 °C, at which reaction kinetics are maximized with no damage done to the catalyst structure and acidity [95]. Even though an increase in temperature will enhance olefin activation and product formation, it will also increase the rate of undesired side reactions, such as oligomerization, cracking, and coke formation, causing catalyst deactivation to occur more rapidly [228]. The use of the aromatic-to-olefin molar ratio is very sensitive to product distribution, and in LAB production, ratios of 5:1 to 10:1 are widely used to minimize polyalkylation, enhance product linearity, and facilitate selectivity towards the mono-alkylated aromatics [21]. In addition to traditional optimization, other process intensification methods are becoming popular, like the implementation of microreactors and continuous-flow systems. Their large surface-to-volume ratios allow them to conduct efficient heat and mass transfer, maintain strict control over temperature and reduce diffusion constraints, which is especially useful in acid-catalyzed alkylation reactions [229]. In comparison to traditional batch or fixed-bed reactors, continuous-flow microreactors have better homogeneity of reactions, increased safety, lower catalyst inventory, reduced environmental impact, and easier scale-up, and can thus greatly enhance the efficiency and sustainability of a process [165].

Table 6. Economic comparison of alkylation technologies [230].

Technology	Initial Investment	Operating Cost	Catalyst Life	Environmental Impact	Product Quality
HF-based	Low	High	Continuous	High	Excellent
$AlCl_3$-based	Low	High	Continuous	High	Good
Zeolite-based	Medium	Low	6–12 months	Low	Excellent
Modified Zeolite	Medium-High	Low	12–24 months	Very Low	Excellent

10. Future Directions and Emerging Technologies

The upcoming generation of zeolite-based catalysts is increasingly defining contemporary industrial alkylation reactions because of their improved coke resistance, greater regenerability, and structural flexibility [231]. A key area of study is the synthesis of hierarchical zeolites having customized pore structures, integrating the shape selectivity of micro-pores with enhanced mass-transfer characteristics of mesopores [90,232]. These systems substantially reduce diffusion constraints, reduce coke build-ups and increase the lifetime of catalysts in harsh working environments. Simultaneously, metal-modified zeolites are becoming a subject of significant interest because the introduction or encapsulation of metal species provides extra-functionalities and enhances catalytic activities [75,233]. Interestingly, the cerium-modified zeolites have been found to show significantly improved activity, stability and coke resistance, as well as acid modulation and proton transfer efficiency, which are attributed to the synergistic interaction between Brunsten acid sites and metal centers [234–236]. In addition to the continued development of experimental methods, computational methods are increasingly becoming significant in the development of catalysts. Density functional theory (DFT) allows one to study reaction energetics, coke-formation pathways, diffusion barriers, and structure-activity relationships in great detail [221]. Machine-learning and data-based models also help speed up catalyst screening and performance prediction by a considerable margin of experimental effort and time to develop [222,237]. Hierarchical design, metal engineering and computation-guided catalyst engineering are therefore a potent approach to designing zeolite catalysts with activity, selectivity, stability, and sustainability never before seen in aromatic alkylation technology in the future [114,148].

11. Conclusions

This review has examined the importance of coke formation during aromatic alkylation reactions over dealuminated and desilicated HY zeolite catalysts. Zeolite catalysts represent superior alternatives to conventional homogeneous acid catalysts, offering significant advantages in terms of environmental impact, safety, and process economics. The evidence clearly shows that structural modifications through dealumination and desilication are powerful strategies for optimizing catalyst properties. Adjusting the strength and concentration of acid sites via dealumination, combined with the introduction of mesoporosity through desilication, enhances mass transfer and reduces diffusion limitations.

Such integrated treatments yield hierarchical zeolites with optimized activity–selectivity–stability profiles, achieving a LAB selectivity above 90% and enabling long-lived catalytic systems. Future research should focus on developing the next generation of hierarchical zeolites with improved coke tolerance, implementing sustainable regeneration technologies, and applying advanced digital tools to optimize catalytic processes. These innovations will remain essential for creating environmentally benign chemical processes capable of meeting the increasing industrial demands while maintaining economic viability and high product quality.

Author Contributions: Conceptualization, B.Y.A.-Z. and A.A.-S.; validation, A.A.A.-S. and A.A.-S.; formal analysis, B.Y.A.-Z. and A.A.-S.; investigation, A.A.A.-S. and B.Y.A.-Z.; resources, A.A.A.-S. and A.A.-S.; data curation, A.A.A.-S. and A.A.-S.; writing—original draft preparation, A.A.A.-S. and A.A.-S.; writing—review and editing, A.A.A.-S., B.Y.A.-Z. and A.A.-S.; visualization, A.A.A.-S.; supervision, B.Y.A.-Z. and A.A.-S.; project administration, A.A.-S.; funding acquisition, A.A.A.-S. All authors have read and agreed to the published version of the manuscript.

Funding: This research received no external funding.

Data Availability Statement: No new data were created or analyzed in this study. Data sharing is not applicable to this article.

Conflicts of Interest: We certify that we have no affiliations with or involvement in any organization or entity with any financial interest or nonfinancial interest in the subject matter or materials discussed in this manuscript.

References

1. Li, T.; Shoinkhorova, T.; Gascon, J.; Ruiz-Martínez, J. Aromatics Production via Methanol-Mediated Transformation Routes. *ACS Catal.* **2021**, *11*, 7780–7819. [CrossRef]
2. Al-Sultani, S.H.; Al-Shathr, A.; Al-Zaidi, B.Y. Aromatics Alkylated with Olefins Utilizing Zeolites as Heterogeneous Catalysts: A Review. *Reactions* **2024**, *5*, 900–927. [CrossRef]
3. Fals, J.; Toloza, C.A.T.; Puello-Polo, E.; Márquez, E.; Méndez, F.J. A comprehensive study of product distributions and coke deposition during catalytic cracking of vacuum gas oil over hierarchical zeolites. *Heliyon* **2023**, *9*, e15408. [CrossRef]
4. Imarc. *Linear Alkylbenzene (LAB) Market Size, Share, Trends and Forecast by Application, End User, and Region, 2025–2033*; Market Reports World: Pune, India, 2024.
5. Fan, S.; Wang, H.; Wang, P.; Jiao, W.; Wang, S.; Qin, Z.; Dong, M.; Wang, J.; Fan, W. Formation and evolution of the coke precursors on the zeolite catalyst in the conversion of methanol to olefins. *Chem Catal.* **2024**, *4*, 100927. [CrossRef]
6. Mtui, H.I.; Wang, W.; Yang, S.-Z.; Mu, B.-Z. Structural diversity and properties of bio-based surfactants with their potential applications. *Bioresour. Technol.* **2026**, *440*, 133509. [CrossRef] [PubMed]
7. Shokri, A.; Karimi, S. A Review in Linear Alkylbenzene (LAB) Production Processes in the Petrochemical Industry. *Russ. J. Appl. Chem.* **2021**, *94*, 1546–1559. [CrossRef]
8. Badmus, S.O.; Amusa, H.K.; Oyehan, T.A.; Saleh, T.A. Environmental risks and toxicity of surfactants: Overview of analysis, assessment, and remediation techniques. *Environ. Sci. Pollut. Res.* **2021**, *28*, 62085–62104. [CrossRef]
9. Vogt, E.T.C.; Fu, D.; Weckhuysen, B.M. Carbon Deposit Analysis in Catalyst Deactivation, Regeneration, and Rejuvenation. *Angew. Chem. Int. Ed. Engl.* **2023**, *62*, e202300319. [CrossRef]
10. Horňáček, M.; Bérešová, M.; Hudec, P. An Environmentally Friendly Catalyst for Aromatic Hydrocarbons Alkylations with 1-alkenes. *WSEAS Trans. Environ. Dev.* **2024**, *20*, 835–843. [CrossRef]
11. Sun, Y.; Wei, L.; Zhang, Z.; Zhang, H.; Li, Y. Coke Formation over Zeolite Catalysts in Light Alkanes Aromatization and Anti-Carbon-Deposition Strategies and Perspectives: A Review. *Energy Fuels* **2023**, *37*, 1657–1677. [CrossRef]
12. Al-Shathr, A.; Al-Zaidi, B.Y.; Aal-Kaeb, S.; Shakor, Z.M.; Majdi, H.S.; Alsaffar, M.A.; Al-Saedy, M.A.E.; Jassem, A.M.; Hamied, R.S.; Al-Zuhairi, F.K.; et al. Investigation of toluene alkylation with hept-1-ene over fresh and modified h-beta catalysts according to apparent activation energy values. *S. Afr. J. Chem. Eng.* **2025**, *54*, 114–132. [CrossRef]
13. Parangi, T. Heterogeneous catalysis: An alternative approach for energy and environment. *Rev. Inorg. Chem.* **2025**, *45*, 831–861. [CrossRef]
14. Zormpa, F.; Treu, P.; Saraçi, E. Advancing biomass valorization with zeolite catalysts: Focus on oxidative transformations. *Sustain. Chem. Environ.* **2025**, *10*, 100249. [CrossRef]
15. Hua, J.; Ji, M.; Jiao, P.; Yin, Z.; Xia, Q.; Jiang, L.; Zhang, J.; Pan, H. Heterogeneous Acid Catalysts for Biodiesel Production: Effect of Physicochemical Properties on Their Activity and Reusability. *Catalysts* **2025**, *15*, 396. [CrossRef]
16. Zhang, H.; bin Samsudin, I.b.; Jaenicke, S.; Chuah, G.-K. Zeolites in catalysis: Sustainable synthesis and its impact on properties and applications. *Catal. Sci. Technol.* **2022**, *12*, 6024–6039. [CrossRef]
17. Ali, N.S.; Salih, I.K.; Harharah, H.N.; Majdi, H.S.; Salih, H.G.; Kalash, K.R.; Al-Shathr, A.; Al-Sudani, F.T.; Abdulrahman, M.A.; Alrubaye, J.M.; et al. Utilization of Loaded Cobalt onto MCM-48 Mesoporous Catalyst as a Heterogeneous Reaction in a Fixed Bed Membrane Reactor to Produce Isomerization Product from n-Heptane. *Catalysts* **2023**, *13*, 1138. [CrossRef]
18. Azam, M.U.; Fernandes, A.; Ferreira, M.J.; Afzal, W.; Graça, I. Pore-Structure Engineering of Hierarchical β Zeolites for the Enhanced Hydrocracking of Waste Plastics to Liquid Fuels. *ACS Catal.* **2024**, *14*, 16148–16165. [CrossRef]
19. Abdul-Kader, H.A.; Shakor, Z.M.; Sherhan, B.Y.; Al-Humairi, S.T.; Aboughaly, M.; Hazrat, M.A.; Fattah, I.M.R. Biodiesel production from waste cooking oil using KOH/HY-type nano-catalyst derived from silica sand. *Biofuels* **2024**, *15*, 527–543. [CrossRef]
20. Al-Sultani, S.H.; Al-Shathr, A.; Al-Zaidi, B.Y.; Shakor, Z.M.; Al-Shafei, E. Sustainable Liquid-Phase Alkylation of Toluene Using Zeolitic Catalysts: A Comparative Evaluation of Al-Rich Y and Si-Rich Beta Zeolites for Industrial Green Chemistry to Support Sustainable Development Goals (SDGs). *ASEAN J. Sci. Eng.* **2025**, *6*, 209–232.
21. Al-Sultani, S.H.; Al-Shathr, A.; Al-Zaidi, B.Y. Toluene Alkylation Reactions over Y-Type Zeolite Catalysts: An Experimental and Kinetic Study. *Reactions* **2024**, *5*, 1042–1065. [CrossRef]

22. Khan, W.; Jia, X.; Wu, Z.; Choi, J.; Yip, A.C.K. Incorporating Hierarchy into Conventional Zeolites for Catalytic Biomass Conversions: A Review. *Catalysts* **2019**, *9*, 127. [CrossRef]
23. Al-Shathr, A.; Al-Zaidi, B.Y.; Shehab, A.K.; Shakoor, Z.M.; Aal-Kaeb, S.; Gomez, L.Q.; Majdi, H.S.; Al-Shafei, E.N.; AbdulRazak, A.A.; McGregor, J. Experimental and kinetic studies of the advantages of coke accumulation over Beta and Mordenite catalysts according to the pore mouth catalysis hypothesis. *Catal. Commun.* **2023**, *181*, 106718. [CrossRef]
24. Al-Zaidi, B.Y.; Al-Shathr, A.; Shehab, A.K.; Shakor, Z.M.; Majdi, H.S.; AbdulRazak, A.A.; McGregor, J. Hydroisomerisation and Hydrocracking of n-Heptane: Modelling and Optimisation Using a Hybrid Artificial Neural Network–Genetic Algorithm (ANN–GA). *Catalysts* **2023**, *13*, 1125. [CrossRef]
25. Al-Zaidi, B.Y.; Holmes, R.J.; Garforth, A.A. Study of the Relationship between Framework Cation Levels of Y Zeolites and Behavior during Calcination, Steaming, and n-Heptane Cracking Processes. *Ind. Eng. Chem. Res.* **2012**, *51*, 6648–6657. [CrossRef]
26. Perego, C.; Ingallina, P. Recent advances in the industrial alkylation of aromatics: New catalysts and new processes. *Catal. Today* **2002**, *73*, 3–22. [CrossRef]
27. Zhu, X.; Gao, Y.; Chen, H.; Jiang, M.; Wang, X.; Miao, C.; Shen, Y.; Ji, Y.; Qin, Z.; Wu, Z.; et al. Constructing Hierarchical Zeolites with Highly Complete Framework via Controlled Desilication. *Angew. Chem. Int. Ed. Engl.* **2024**, *63*, e202411446. [CrossRef]
28. Oliveira, D.S.; Lima, R.B.; Pergher, S.B.C.; Caldeira, V.P.S. Hierarchical Zeolite Synthesis by Alkaline Treatment: Advantages and Applications. *Catalysts* **2023**, *13*, 316. [CrossRef]
29. Shakor, Z.; Alasseel, A.; Al-Shafei, E. The structure of deposited coke on hydrocracking and reforming catalysts: Coke deactivation and kinetics. *Can. J. Chem. Eng.* **2024**, *102*, 2876–2891. [CrossRef]
30. Guisnet, M.; Ribeiro, F.R. *Deactivation and Regeneration of Zeolite Catalysts*; Imperial College Press: London, UK, 2011.
31. Collett, C.H.; McGregor, J. Things go better with coke: The beneficial role of carbonaceous deposits in heterogeneous catalysis. *Catal. Sci. Technol.* **2015**, *6*, 363–378. [CrossRef]
32. Bahlouli, H.A.; Alghamdi, R.; Manos, G. Coke Characterization and Re-Activation Energy Dynamics of Spent FCC Catalyst in the Catalytic Pyrolysis of Polyolefins. *Catalysts* **2025**, *15*, 862. [CrossRef]
33. Guisnet, M.; Pinard, L. Characterization of acid-base catalysts through model reactions. *Catal. Rev.* **2018**, *60*, 337–436. [CrossRef]
34. Mohammed, M.I.; Abdul Razak, A.A.; Shehab, M.A. Synthesis of Nanocatalyst for Hydrodesulfurization of Gasoil Using Laboratory Hydrothermal Rig. *Arab. J. Sci. Eng.* **2017**, *42*, 1381–1387. [CrossRef]
35. Spivey, J.J.; Roberts, G.W.; Querini, C.A.; Sanati, M.; Kogelbauer, A.; Margitfalvi, J.L.; Hutchings, G.J.; Kung, H.H.; Querini, C.; Boutonnet, M.; et al. Coke characterization. In *Catalysis*; Spivey, J.J., Roberts, G.W., Eds.; The Royal Society of Chemistry: London, UK, 2004; Volume 17, pp. 166–206.
36. Schmidt, J.E.; Poplawsky, J.D.; Mazumder, B.; Attila, Ö.; Fu, D.; de Winter, D.A.M.; Meirer, F.; Bare, S.R.; Weckhuysen, B.M. Coke Formation in a Zeolite Crystal During the Methanol-to-Hydrocarbons Reaction as Studied with Atom Probe Tomography. *Angew. Chem.* **2016**, *128*, 11339–11343. [CrossRef]
37. Qin, Z.; Zeng, S.; Melinte, G.; Bučko, T.; Badawi, M.; Shen, Y.; Gilson, J.P.; Ersen, O.; Wei, Y.; Liu, Z.; et al. Understanding the Fundamentals of Microporosity Upgrading in Zeolites: Increasing Diffusion and Catalytic Performances. *Adv. Sci.* **2021**, *8*, 2100001. [CrossRef]
38. Zwain, A.; Al-Zaidi, B.; Shakor, Z.M.; Al-Shathr, A.; Al-Shafei, E. Low-Pressure Hydrodesulfurization Catalysts of Heavy Gas Oil Using Activated Bentonite and Kaolin Clay Supports. *ACS Omega* **2025**, *10*, 36917–36930. [CrossRef] [PubMed]
39. Hessou, E.P.; Ponce-Vargas, M.; Mensah, J.-B.; Tielens, F.; Santos, J.C.; Badawi, M. Dibenzyl Disulfide Adsorption on Cationic Exchanged Faujasites: A DFT Study. *Nanomaterials* **2019**, *9*, 715. [CrossRef]
40. Wu, D.; Yang, M.; Yu, J.; Dyballa, M.; Yang, P.; Li, M.; Hou, G.; Hunger, M.; Dai, W. The role of adsorption and diffusion in improving the selectivity and reactivity of zeolite catalysts. *Chem. Soc. Rev.* **2025**, *54*, 9192–9244. [CrossRef]
41. Qin, Z.; Cychosz, K.A.; Melinte, G.; El Siblani, H.; Gilson, J.P.; Thommes, M.; Fernandez, C.; Mintova, S.; Ersen, O.; Valtchev, V. Opening the Cages of Faujasite-Type Zeolite. *J. Am. Chem. Soc.* **2017**, *139*, 17273–17276. [CrossRef]
42. Castoldi, L.; Morandi, S.; Ticali, P.; Matarrese, R.; Lietti, L. An Assessment of Zeolite Framework Effect for Low-Temperature NOX Adsorbers. *Catalysts* **2023**, *13*, 962. [CrossRef]
43. Astafan, A.; Sachse, A.; Batiot-Dupeyrat, C.; Pinard, L. Impact of the Framework Type on the Regeneration of Coked Zeolites by Non-Thermal Plasma in a Fixed Bed Dielectric Barrier Reactor. *Catalysts* **2019**, *9*, 985. [CrossRef]
44. Craciun, I.; Reyniers, M.-F.; Marin, G.B. Effects of acid properties of Y zeolites on the liquid-phase alkylation of benzene with 1-octene: A reaction path analysis. *J. Mol. Catal. A Chem.* **2007**, *277*, 1–14. [CrossRef]
45. Daligaux, V.; Richard, R.; Manero, M.-H. Deactivation and Regeneration of Zeolite Catalysts Used in Pyrolysis of Plastic Wastes—A Process and Analytical Review. *Catalysts* **2021**, *11*, 770. [CrossRef]
46. Wei, L.; Wang, H.; Dong, Q.; Li, Y.; Xiang, H. A Review on the Research Progress of Zeolite Catalysts for Heavy Oil Cracking. *Catalysts* **2025**, *15*, 401. [CrossRef]

47. Manrique, C.; Botero, T.; Solano, R.; Mendoza, C.; Echavarría-Isaza, A. Efficient synthesis of nanosized zeolite Y utilizing gradual heating: Post-synthesis modification and their catalytic performance in propylene oligomerization. *J. Porous Mater.* **2025**, *32*, 1039–1056. [CrossRef]
48. Vasconcelos, A.A.; Len, T.; de Oliveira, A.d.N.; da Costa, A.A.F.; da Silva Souza, A.R.; da Costa, C.E.F.; Luque, R.; da Rocha Filho, G.N.; Noronha, R.C.R.; do Nascimento, L.A.S. Zeolites: A Theoretical and Practical Approach with Uses in (Bio)Chemical Processes. *Appl. Sci.* **2023**, *13*, 1897. [CrossRef]
49. Rodríguez-González, L.; Hermes, F.; Bertmer, M.; Rodríguez-Castellón, E.; Jiménez-López, A.; Simon, U. The acid properties of H-ZSM-5 as studied by NH3-TPD and 27Al-MAS-NMR spectroscopy. *Appl. Catal. A Gen.* **2007**, *328*, 174–182. [CrossRef]
50. Kordala, N.; Wyszkowski, M. Zeolite Properties, Methods of Synthesis, and Selected Applications. *Molecules* **2024**, *29*, 1069. [CrossRef] [PubMed]
51. Kamimura, Y.; Kodaira, T.; Yamada, H.; Hiyoshi, N.; Endo, A. Direct Visualization of the Dealumination Process on Zeolite Y: How Was the Mesoporous Architecture Formed? *Chem. Mater.* **2025**, *37*, 2735–2748. [CrossRef]
52. Zang, J.; Yu, H.; Liu, G.; Hong, M.; Liu, J.; Chen, T. Research Progress on Modifications of Zeolite Y for Improved Catalytic Properties. *Inorganics* **2023**, *11*, 22. [CrossRef]
53. Sun, Q.; Wang, N.; Yu, J. Advances in Catalytic Applications of Zeolite-Supported Metal Catalysts. *Adv. Mater.* **2021**, *33*, 2104442. [CrossRef]
54. Roth, W.J.; Gil, B.; Tarach, K.A.; Góra-Marek, K. Top-down engineering of zeolite porosity. *Chem. Soc. Rev.* **2025**, *54*, 7484–7560. [CrossRef]
55. Yilmaz, B.; Müller, U. Catalytic Applications of Zeolites in Chemical Industry. *Top. Catal.* **2009**, *52*, 888–895. [CrossRef]
56. Sivagami, K.; Kumar, K.V.; Tamizhdurai, P.; Govindarajan, D.; Kumar, M.; Nambi, I. Conversion of plastic waste into fuel oil using zeolite catalysts in a bench-scale pyrolysis reactor. *RSC Adv.* **2022**, *12*, 7612–7620. [CrossRef]
57. Guisnet, M.; Gilson, J.-P. *Zeolites for Cleaner Technologies*; Hutchings, G.J., Ed.; Imperial College Press: London, UK, 2002; Volume 3.
58. Yi, X.; Peng, Y.-K.; Chen, W.; Liu, Z.; Zheng, A. Surface Fingerprinting of Faceted Metal Oxides and Porous Zeolite Catalysts by Probe-Assisted Solid-State NMR Approaches. *Acc. Chem. Res.* **2021**, *54*, 2421–2433. [CrossRef] [PubMed]
59. Yoshioka, T.; Iyoki, K.; Hotta, Y.; Kamimura, Y.; Yamada, H.; Han, Q.; Kato, T.; Fisher, C.A.J.; Liu, Z.; Ohnishi, R.; et al. Dealumination of small-pore zeolites through pore-opening migration process with the aid of pore-filler stabilization. *Sci. Adv.* **2022**, *8*, eabo3093. [CrossRef]
60. Karpe, S.; Veser, G. Coke Formation and Regeneration during Fe-ZSM-5-Catalyzed Methane Dehydro-Aromatization. *Catalysts* **2024**, *14*, 292. [CrossRef]
61. Yan, P.; Wang, H.; Liao, Y.; Wang, C. Zeolite catalysts for the valorization of biomass into platform compounds and biochemicals/biofuels: A review. *Renew. Sustain. Energy Rev.* **2023**, *178*, 113219. [CrossRef]
62. Bai, R.; Song, Y.; Li, Y.; Yu, J. Creating Hierarchical Pores in Zeolite Catalysts. *Trends Chem.* **2019**, *1*, 601–611. [CrossRef]
63. Li, W.; Zheng, J.; Luo, Y.; Tu, C.; Zhang, Y.; Da, Z. Hierarchical Zeolite Y with Full Crystallinity: Formation Mechanism and Catalytic Cracking Performance. *Energy Fuels* **2017**, *31*, 3804–3811. [CrossRef]
64. Wei, Y.; Parmentier, T.E.; de Jong, K.P.; Zečević, J. Tailoring and visualizing the pore architecture of hierarchical zeolites. *Chem. Soc. Rev.* **2015**, *44*, 7234–7261. [CrossRef]
65. Cundy, C.S.; Cox, P.A. The Hydrothermal Synthesis of Zeolites: History and Development from the Earliest Days to the Present Time. *Chem. Rev.* **2003**, *103*, 663–702. [CrossRef]
66. Feliczak-Guzik, A. Hierarchical zeolites: Synthesis and catalytic properties. *Microporous Mesoporous Mater.* **2018**, *259*, 33–45. [CrossRef]
67. Khaleque, A.; Alam, M.M.; Hoque, M.; Mondal, S.; Haider, J.B.; Xu, B.; Johir, M.A.H.; Karmakar, A.K.; Zhou, J.L.; Ahmed, M.B.; et al. Zeolite synthesis from low-cost materials and environmental applications: A review. *Environ. Adv.* **2020**, *2*, 100019. [CrossRef]
68. Luo, Y.; Fu, W.; Wang, B.; Yuan, Z.; Sun, J.; Zou, X.; Yang, W. SCM-25: A Zeolite with Ordered Meso-cavities Interconnected by 12 × 12 × 10-Ring Channels Determined by 3D Electron Diffraction. *Inorg. Chem.* **2022**, *61*, 4371–4377. [CrossRef]
69. Liu, Z.; Yuan, J.; van Baten, J.M.; Zhou, J.; Tang, X.; Zhao, C.; Chen, W.; Yi, X.; Krishna, R.; Sastre, G.; et al. Synergistically enhance confined diffusion by continuum intersecting channels in zeolites. *Sci. Adv.* **2021**, *7*, eabf0775. [CrossRef]
70. Kunz, L.Y.; Bu, L.; Knott, B.C.; Liu, C.; Nimlos, M.R.; Assary, R.S.; Curtiss, L.A.; Robichaud, D.J.; Kim, S. Theoretical Determination of Size Effects in Zeolite-Catalyzed Alcohol Dehydration. *Catalysts* **2019**, *9*, 700. [CrossRef]
71. Li, J.; Gao, M.; Yan, W.; Yu, J. Regulation of the Si/Al ratios and Al distributions of zeolites and their impact on properties. *Chem. Sci.* **2023**, *14*, 1935–1959. [CrossRef]
72. Marino, A.; Catizzone, E.; Migliori, M.; Ferrarelli, G.; Aloise, A.; Chillè, D.; Papanikolaou, G.; Lanzafame, P.; Perathoner, S.; Centi, G.; et al. Hydrothermal Synthesis and Catalytic Assessment of High-Silica (B,Fe)-beta Zeolites. *Cryst. Growth Des.* **2023**, *23*, 2988–3001. [CrossRef]

73. Zvereva, I.A.; Shelyapina, M.G.; Chislov, M.; Novakowski, V.; Malygina, E.; Rodríguez-Iznaga, I.; Hernández, M.-A.; Petranovskii, V. A comparative analysis of natural zeolites from various Cuban and Mexican deposits: Structure, composition, thermal properties and hierarchical porosity. *J. Therm. Anal. Calorim.* **2022**, *147*, 6147–6159. [CrossRef]
74. Zhang, S.; Gan, S.; Liu, B.; Dong, J. Production of linear alkylbenzene over Ce containing Beta zeolites. *Chin. J. Chem. Eng.* **2024**, *67*, 220–227. [CrossRef]
75. Zhu, T.; Zhang, T.; Xiao, L.; Zhang, C.; Li, Y. Synthesis and Applications of Zeolite-Encapsulated Metal Catalysts. *Catalysts* **2025**, *15*, 836. [CrossRef]
76. Xing, S.; Liu, X.; Cui, Y.; Zhao, Y.; Chen, Z.; Xiang, S.; Han, M. Elucidating the deactivation mechanism of beta zeolite catalyzed linear alkylbenzene production with oxygenated organic compound contaminated feedstocks. *RSC Adv.* **2024**, *14*, 9243–9253. [CrossRef]
77. Navarro de Miguel, J.C.; Chung, S.-H.; Dikhtiarenko, A.; Li, T.; Patarroyo, J.; Ruiz-Martínez, J. Brønsted Acid-Site Density Controls the Mechanistic Cycle and Product Selectivity in the Methanol-to-Hydrocarbons Reaction in BEA Zeolite. *ACS Catal.* **2024**, *14*, 5989–6000. [CrossRef]
78. Melchionna, M.; Fornasiero, P. The role of ceria/precious metal interfaces in catalysis. *RSC Appl. Interfaces* **2024**, *1*, 70–79. [CrossRef]
79. Meiramkulova, K.; Kydyrbekova, A.; Devrishov, D.; Nurbala, U.; Tuyakbayeva, A.; Zhangazin, S.; Ualiyeva, R.; Kolpakova, V.; Yeremeyeva, Y.; Mkilima, T. Comparative Analysis of Natural and Synthetic Zeolite Filter Performance in the Purification of Groundwater. *Water* **2023**, *15*, 588. [CrossRef]
80. Fu, D.; Maris, J.J.E.; Stanciakova, K.; Nikolopoulos, N.; van der Heijden, O.; Mandemaker, L.D.B.; Siemons, M.E.; Salas Pastene, D.; Kapitein, L.C.; Rabouw, F.T.; et al. Unravelling Channel Structure–Diffusivity Relationships in Zeolite ZSM-5 at the Single-Molecule Level. *Angew. Chem. Int. Ed. Engl.* **2022**, *61*, e202114388. [CrossRef]
81. Seremak, A.; Capel Berdiell, I.; Arstad, B.; Fjermestad, T.; Svelle, S. Investigating the Flexibility of H-ZSM-5 Zeolite Upon Adsorption of Coke Precursors: A Theoretical and Experimental Approach. *J. Phys. Chem. C* **2025**, *129*, 1183–1197. [CrossRef] [PubMed]
82. Wang, H.; Shen, B.; Chen, X.; Xiong, H.; Wang, H.; Song, W.; Cui, C.; Wei, F.; Qian, W. Modulating inherent lewis acidity at the intergrowth interface of mortise-tenon zeolite catalyst. *Nat. Commun.* **2022**, *13*, 2924. [CrossRef]
83. Li, Y.; Wang, H.; Dong, M.; Li, J.; Qin, Z.; Wang, J.; Fan, W. Effect of zeolite pore structure on the diffusion and catalytic behaviors in the transalkylation of toluene with 1,2,4-trimethylbenzene. *RSC Adv.* **2015**, *5*, 66301–66310. [CrossRef]
84. Hou, Y.; Li, X.; Sun, M.; Li, C.; Bakhtiar, S.U.H.; Lei, K.; Yu, S.; Wang, Z.; Hu, Z.; Chen, L.; et al. The effect of hierarchical single-crystal ZSM-5 zeolites with different Si/Al ratios on its pore structure and catalytic performance. *Front. Chem. Sci. Eng.* **2021**, *15*, 269–278. [CrossRef]
85. Mancinelli, M.; Precisvalle, N.; Ardit, M.; Beltrami, G.; Gigli, L.; Catizzone, E.; Migliori, M.; Giordano, G.; Martucci, A. Thermal stability of templated ZSM-5 zeolites: An in-situ synchrotron X-ray powder diffraction study. *Microporous Mesoporous Mater.* **2023**, *362*, 112777. [CrossRef]
86. Rajaei, H.; Esmaeilzadeh, F.; Mowla, D. Elucidation of Si/Al ratio on physicochemical properties of HZSM-5 zeolites. *J. Therm. Anal. Calorim.* **2021**, *146*, 581–586. [CrossRef]
87. Kokotailo, G.T.; Lawton, S.L.; Olson, D.H.; Meier, W.M. Structure of synthetic zeolite ZSM-5. *Nature* **1978**, *272*, 437–438. [CrossRef]
88. Jangkorn, S.; Youngme, S.; Praipipat, P. Comparative lead adsorptions in synthetic wastewater by synthesized zeolite A of recycled industrial wastes from sugar factory and power plant. *Heliyon* **2022**, *8*, e09323. [CrossRef]
89. Pérez-Botella, E.; Valencia, S.; Rey, F. Zeolites in Adsorption Processes: State of the Art and Future Prospects. *Chem. Rev.* **2022**, *122*, 17647–17695. [CrossRef] [PubMed]
90. Hijazi, N.; Bavykina, A.; Yarulina, I.; Shoinkhorova, T.; Ramos-Fernandez, E.V.; Gascon, J. Chemical engineering of zeolites: Alleviating transport limitations through hierarchical design and shaping. *Chem. Soc. Rev.* **2025**, *54*, 6335–6384. [CrossRef]
91. Da, Z.; Han, Z.; Magnoux, P.; Guisnet, M. Liquid-phase alkylation of toluene with long-chain alkenes over HFAU and HBEA zeolites. *Appl. Catal. A Gen.* **2001**, *219*, 45–52. [CrossRef]
92. Wei, Y.; Feng, J.; Guan, B.; Yu, J. Structural Engineering of Hierarchical Zeolite-Based Catalysts. *Acc. Mater. Res.* **2024**, *5*, 857–871. [CrossRef]
93. Bailleul, S.; Yarulina, I.; Hoffman, A.E.J.; Dokania, A.; Abou-Hamad, E.; Chowdhury, A.D.; Pieters, G.; Hajek, J.; De Wispelaere, K.; Waroquier, M.; et al. A Supramolecular View on the Cooperative Role of Brønsted and Lewis Acid Sites in Zeolites for Methanol Conversion. *J. Am. Chem. Soc.* **2019**, *141*, 14823–14842. [CrossRef]
94. Bigi, F.; Carloni, S.; Flego, C.; Maggi, R.; Mazzacani, A.; Rastelli, M.; Sartori, G. HY zeolite-promoted electrophilic acylation of methoxyarenes with linear acid chlorides. *J. Mol. Catal. A Chem.* **2002**, *178*, 139–146. [CrossRef]
95. Baerlocher, C.; McCusker, L.B.; Olson, D.H. *Atlas of Zeolite Framework Types*, 6th ed.; Elsevier: Amsterdam, The Netherlands, 2007.
96. Silaghi, M.-C.; Chizallet, C.; Sauer, J.; Raybaud, P. Dealumination mechanisms of zeolites and extra-framework aluminum confinement. *J. Catal.* **2016**, *339*, 242–255. [CrossRef]

97. Lu, X.; Wei, C.; Zhao, L.; Gao, J.; Xu, C. Modification of the Acidic and Textural Properties of HY Zeolite by AHFS Treatment and Its Coke Formation Performance in the Catalytic Cracking Reaction of N-Butene. *Catalysts* **2022**, *12*, 640. [CrossRef]
98. Manrique, C.; Solano, R.; Mendoza, C.; Amaya, S.; Echavarría, A. Hierarchical submicrosized Y zeolites prepared by sequential desilication–dealumination post-synthesis modification and their catalytic performance in vacuum gas oil hydrocracking. *New J. Chem.* **2024**, *48*, 6188–6200. [CrossRef]
99. Mancuso, J.L.; Van Speybroeck, V. The nature of extraframework aluminum species and Brønsted acid site interactions under catalytic operating conditions. *J. Catal.* **2024**, *429*, 115211. [CrossRef]
100. Li, R.; Lin, Q.; Ren, J.; Yang, X.; Wang, Y.; Kong, L. Dealuminated Hβ zeolite for selective conversion of fructose to furfural and formic acid. *Green Energy Environ.* **2024**, *9*, 311–320. [CrossRef]
101. Zhang, R.; Zhong, P.; Arandiyan, H.; Guan, Y.; Liu, J.; Wang, N.; Jiao, Y.; Fan, X. Using ultrasound to improve the sequential post-synthesis modification method for making mesoporous Y zeolites. *Front. Chem. Sci. Eng.* **2020**, *14*, 275–287. [CrossRef]
102. Volavšek, J.; Pliekhov, O.; Pliekhova, O.; Mali, G.; Zabukovec Logar, N. Study of Water Adsorption on EDTA-Modified LTA Zeolites. *Nanomaterials* **2022**, *12*, 1352. [CrossRef] [PubMed]
103. Zheng, Y.; Espinosa, M.; Mon, M.; Leyva–Pérez, A. Dealuminated H–Y zeolites generate, stabilize and catalytically insert carbenes from diazocarbonyl compounds. *J. Catal.* **2024**, *440*, 115835. [CrossRef]
104. Wang, C.; Brenig, A.; Xu, J.; Deng, F.; Paunović, V.; van Bokhoven, J.A. Evidence of Preferential Aluminum Site Loss during Reaction-Induced Dealumination. *J. Am. Chem. Soc.* **2024**, *146*, 34279–34284. [CrossRef]
105. He, L.-H.; Li, J.-J.; Han, S.-Y.; Fan, D.; Li, X.-J.; Xu, S.-T.; Wei, Y.-X.; Liu, Z.-M. Dynamic evolution of HZSM-5 zeolite framework under steam treatment. *Chem. Synth.* **2024**, *4*, 1. [CrossRef]
106. Khivantsev, K.; Jaegers, N.R.; Kovarik, L.; Derewinski, M.A.; Kwak, J.H.; Szanyi, J. On the Nature of Extra-Framework Aluminum Species and Improved Catalytic Properties in Steamed Zeolites. *Molecules* **2022**, *27*, 2352. [CrossRef]
107. Cao, Z.; Bu, J.; Zhong, Z.; Sun, C.; Zhang, Q.; Wang, J.; Chen, S.; Xie, X. Selective hydrogenation of cinnamaldehyde to cinnamyl alcohol over BN-supported Pt catalysts at room temperature. *Appl. Catal. A Gen.* **2019**, *578*, 105–115. [CrossRef]
108. Hart, A.; Wood, J. Methodological review of zeolite synthesis from industrial waste and natural clays and the fabrication of hierarchical pore structures. *Next Mater.* **2025**, *9*, 101113. [CrossRef]
109. Prodinger, S.; Derewinski, M.A. Recent Progress to Understand and Improve Zeolite Stability in the Aqueous Medium. *Pet. Chem.* **2020**, *60*, 420–436. [CrossRef]
110. Wouters, B.H.; Chen, T.; Grobet, P.J. Steaming of Zeolite Y: Formation of Transient Al Species. *J. Phys. Chem. B* **2001**, *105*, 1135–1139. [CrossRef]
111. Azam, M.U.; Afzal, W.; Fernandes, A.; Graça, I. Insights into the development of greener mild zeolite dealumination routes applied to the hydrocracking of waste plastics. *Appl. Catal. A Gen.* **2024**, *685*, 119873. [CrossRef]
112. Sun, H.; Peng, P.; Wang, Y.; Li, C.; Subhan, F.; Bai, P.; Xing, W.; Zhang, Z.; Liu, Z.; Yan, Z. Preparation, scale-up and application of meso-ZSM-5 zeolite by sequential desilication–dealumination. *J. Porous Mater.* **2017**, *24*, 1513–1525. [CrossRef]
113. Batool, S.R.; Sushkevich, V.L.; van Bokhoven, J.A. Factors Affecting the Generation and Catalytic Activity of Extra-Framework Aluminum Lewis Acid Sites in Aluminum-Exchanged Zeolites. *ACS Catal.* **2024**, *14*, 678–690. [CrossRef]
114. Verboekend, D.; Pérez-Ramírez, J. Design of hierarchical zeolite catalysts by desilication. *Catal. Sci. Technol.* **2011**, *1*, 879–890. [CrossRef]
115. Groen, J.C.; Peffer, L.A.A.; Moulijn, J.A.; Pérez-Ramírez, J. Mechanism of hierarchical porosity development in MFI zeolites by desilication: The role of aluminium as a pore-directing agent. *Chem.—A Eur. J.* **2005**, *11*, 4983–4994. [CrossRef]
116. Liang, D.; Liu, Y.; Zhang, R.; Xie, Q.; Zhang, L. A Review on the Influence Factors in the Synthesis of Zeolites and the Transformation Behavior of Silicon and Aluminum During the Process. *Comments Inorg. Chem.* **2024**, *44*, 461–497. [CrossRef]
117. Mumtaz, F.; Irfan, M.F.; Usman, M.R. Synthesis methods and recent advances in hierarchical zeolites: A brief review. *J. Iran. Chem. Soc.* **2021**, *18*, 2215–2229. [CrossRef]
118. Groen, J.C.; Moulijn, J.A.; Pérez-Ramírez, J. Decoupling mesoporosity formation and acidity modification in ZSM-5 zeolites by sequential desilication–dealumination. *Microporous Mesoporous Mater.* **2005**, *87*, 153–161. [CrossRef]
119. Jin, M.; Liu, M.; Nachtigall, P.; Grajciar, L.; Heard, C.J. Mechanism of Zeolite Hydrolysis under Basic Conditions. *Chem. Mater.* **2021**, *33*, 9202–9212. [CrossRef]
120. Mochizuki, H.; Yokoi, T.; Imai, H.; Namba, S.; Kondo, J.N.; Tatsumi, T. Effect of desilication of H-ZSM-5 by alkali treatment on catalytic performance in hexane cracking. *Appl. Catal. A Gen.* **2012**, *449*, 188–197. [CrossRef]
121. Matias, P.; Sá Couto, C.; Graça, I.; Lopes, J.M.; Carvalho, A.P.; Ramôa Ribeiro, F.; Guisnet, M. Desilication of a TON zeolite with NaOH: Influence on porosity, acidity and catalytic properties. *Appl. Catal. A Gen.* **2011**, *399*, 100–109. [CrossRef]
122. Cheng, C.; Li, G.; Ji, D.; Zhao, Y.; Shen, J. Regulating hierarchical structure and acidity of HZSM-5 for methanol to aromatics via protective desiliconization and external surface modification. *Microporous Mesoporous Mater.* **2021**, *312*, 110784. [CrossRef]
123. Milina, M.; Mitchell, S.; Crivelli, P.; Cooke, D.; Pérez-Ramírez, J. Mesopore quality determines the lifetime of hierarchically structured zeolite catalysts. *Nat. Commun.* **2014**, *5*, 3922. [CrossRef]

124. Groen, J.C.; Zhu, W.; Brouwer, S.; Huynink, S.J.; Kapteijn, F.; Moulijn, J.A.; Pérez-Ramírez, J. Direct Demonstration of Enhanced Diffusion in Mesoporous ZSM-5 Zeolite Obtained via Controlled Desilication. *J. Am. Chem. Soc.* **2007**, *129*, 355–360. [CrossRef]
125. Ma, Z.; Fu, T.; Wang, Y.; Shao, J.; Ma, Q.; Zhang, C.; Cui, L.; Li, Z. Silicalite-1 Derivational Desilication-Recrystallization to Prepare Hollow Nano-ZSM-5 and Highly Mesoporous Micro-ZSM-5 Catalyst for Methanol to Hydrocarbons. *Ind. Eng. Chem. Res.* **2019**, *58*, 2146–2158. [CrossRef]
126. Khatrin, I.; McCue, A.J.; Abdullah, I.; Krisnandi, Y.K. Structural and Surface Modifications of Zeolite to Tailor Its Catalytic Properties. *ChemistrySelect* **2025**, *10*, e04324. [CrossRef]
127. Groen, J.C.; Moulijn, J.A.; Perez-Ramirez, J. Desilication: On the controlled generation of mesoporosity in MFI zeolites. *J. Mater. Chem.* **2006**, *16*, 2121–2131. [CrossRef]
128. Gackowski, M.; Datka, J. Acid Properties of Hierarchical Zeolites Y. *Molecules* **2020**, *25*, 1044. [CrossRef]
129. Tan, L.; Jiao, N.; Bai, X.; Wang, H.; Wang, J.; Wang, H.; Zhang, X. Methods for Preparing Hierarchical Zeolites by Chemical Etching and Their Catalytic Applications: A Review. *Eur. J. Inorg. Chem.* **2023**, *26*, e202300314. [CrossRef]
130. Tsaplin, D.; Gorbunov, D.; Ostroumova, V.; Gorbunov, A.; Wang, K.; Luo, Z.; Egazaryants, S.; Zairov, R.; Maximov, A.; Naranov, E. ZSM-12 zeolite: The influence of post-synthetic acidic and base treatment on its physicochemical properties and activity in m-Xylene isomerization. *J. Porous Mater.* **2025**, *33*, 75–86. [CrossRef]
131. Xu, Y.; Chen, C.; Lan, Y.; Wang, L.; Li, J. Desilication and recycling of alkali-silicate solution seeded with red mud for low-grade bauxite utilization. *J. Mater. Res. Technol.* **2020**, *9*, 7418–7426. [CrossRef]
132. Sun, Y.; Pan, A.; Ma, Y.; Chang, J. Extraction of alumina and silica from high-silica bauxite by sintering with sodium carbonate followed by two-step leaching with water and sulfuric acid. *RSC Adv.* **2023**, *13*, 23254–23266. [CrossRef]
133. Mwase, J.M.; Safarian, J. Desilication of Sodium Aluminate Solutions from the Alkaline Leaching of Calcium-Aluminate Slags. *Processes* **2022**, *10*, 1769. [CrossRef]
134. Pan, X.; Wu, H.; Yu, H.; Bi, S. Precipitation of desilication products in CaO-Na_2O-Al_2O_3-SiO_2-H_2O system based on the Bayer process. *Hydrometallurgy* **2020**, *197*, 105469. [CrossRef]
135. Kumar Parsapur, R.; Hengne, A.M.; Melinte, G.; Refa Koseoglu, O.; Hodgkins, R.P.; Bendjeriou-Sedjerari, A.; Lai, Z.; Huang, K.-W. Post-Synthetic Ensembling Design of Hierarchically Ordered FAU-type Zeolite Frameworks for Vacuum Gas Oil Hydrocracking. *Angew. Chem. Int. Ed.* **2024**, *63*, e202314217. [CrossRef]
136. Přech, J.; Pizarro, P.; Serrano, D.P.; Čejka, J. From 3D to 2D zeolite catalytic materials. *Chem. Soc. Rev.* **2018**, *47*, 8263–8306. [CrossRef]
137. Wang, C.; Li, J.; Wang, X.; Yang, Z.; Huang, K. Preparation of a Hierarchical Pore Zeolite with High-Temperature Calcination and Acid-Base Leaching. *Clays Clay Miner.* **2019**, *67*, 265–274. [CrossRef]
138. Möller, K.; Bein, T. Mesoporosity—A new dimension for zeolites. *Chem. Soc. Rev.* **2013**, *42*, 3689–3707. [CrossRef] [PubMed]
139. Singh, B.K.; Kim, Y.; Kwon, S.; Na, K. Synthesis of Mesoporous Zeolites and Their Opportunities in Heterogeneous Catalysis. *Catalysts* **2021**, *11*, 1541. [CrossRef]
140. Silaghi, M.-C.; Chizallet, C.; Raybaud, P. Challenges on molecular aspects of dealumination and desilication of zeolites. *Microporous Mesoporous Mater.* **2014**, *191*, 82–96. [CrossRef]
141. Yang, S.; Yu, C.; Yu, L.; Miao, S.; Zou, M.; Jin, C.; Zhang, D.; Xu, L.; Huang, S. Bridging Dealumination and Desilication for the Synthesis of Hierarchical MFI Zeolites. *Angew. Chem. Int. Ed. Engl.* **2017**, *56*, 12553–12556. [CrossRef]
142. Farsana, O.P.; Kumari, P. Hierarchical Assembly of Zeolites: A Present Scenario. *Eng. Sci.* **2023**, *21*, 781. [CrossRef]
143. Wang, Y.; Yokoi, T.; Namba, S.; Tatsumi, T. Effects of Dealumination and Desilication of Beta Zeolite on Catalytic Performance in n-Hexane Cracking. *Catalysts* **2016**, *6*, 8. [CrossRef]
144. Wojciechowska, K. The influence of desilication/dealumination processes on the physicochemical properties of clinoptilolite. *Clay Miner.* **2019**, *54*, 111–119. [CrossRef]
145. Bolshakov, A.; Kosinov, N.; Romero Hidalgo, D.E.; Mezari, B.; van Hoof, A.J.F.; Hensen, E.J.M. Mild dealumination of template-stabilized zeolites by NH4F. *Catal. Sci. Technol.* **2019**, *9*, 4239–4247. [CrossRef]
146. Hasan, Z.; Jun, J.W.; Kim, C.-U.; Jeong, K.-E.; Jeong, S.-Y.; Jhung, S.H. Desilication of ZSM-5 zeolites for mesoporosity development using microwave irradiation. *Mater. Res. Bull.* **2015**, *61*, 469–474. [CrossRef]
147. Han, Y.; Larmier, K.; Rivallan, M.; Pirngruber, G.D. Generation of mesoporosity in H–Y zeolites by basic or acid/basic treatments: Towards a guideline of optimal Si/Al ratio and basic reagent. *Microporous Mesoporous Mater.* **2024**, *365*, 112906. [CrossRef]
148. Zheng, Y.; Ning, W.; Wang, Q.; Wei, X.; Li, X.; Pan, M. Hierarchical ZSM-5 zeolite using amino acid as template: Avoiding phase separation and fabricating an ultra-small mesoporous structure. *Microporous Mesoporous Mater.* **2023**, *355*, 112578. [CrossRef]
149. Wu, L.; Li, Y.; Fu, Z.; Su, B.-L. Hierarchically structured porous materials: Synthesis strategies and applications in energy storage. *Natl. Sci. Rev.* **2020**, *7*, 1667–1701. [CrossRef]
150. Zhou, D.-D.; Du, Y.-J.; Song, Y.-F.; Wang, Y.-G.; Wang, C.-X.; Xia, Y.-Y. Ordered hierarchical mesoporous/microporous carbon with optimized pore structure for supercapacitors. *J. Mater. Chem. A* **2013**, *1*, 1192–1200. [CrossRef]

151. Peng, P.; Gao, X.H.; Yan, Z.F.; Mintova, S. Diffusion and catalyst efficiency in hierarchical zeolite catalysts. *Natl. Sci. Rev.* **2020**, *7*, 1726–1742. [CrossRef]
152. Pérez-Ramírez, J.; Christensen, C.H.; Egeblad, K.; Christensen, C.H.; Groen, J.C. Hierarchical zeolites: Enhanced utilisation of microporous crystals in catalysis by advances in materials design. *Chem. Soc. Rev.* **2008**, *37*, 2530–2542. [CrossRef] [PubMed]
153. Schneider, D.; Mehlhorn, D.; Zeigermann, P.; Kärger, J.; Valiullin, R. Transport properties of hierarchical micro–mesoporous materials. *Chem. Soc. Rev.* **2016**, *45*, 3439–3467. [CrossRef] [PubMed]
154. Wang, Y.; Ren, F.-f.; Pan, D.-h.; Ma, J.-h. A Hierarchically Micro-Meso-Macroporous Zeolite CaA for Methanol Conversion to Dimethyl Ether. *Crystals* **2016**, *6*, 155. [CrossRef]
155. Xu, B.; Deng, M.; Lin, K.; Wang, Y.; Lu, X.; Ma, R.; Fu, Y.; Zhu, W. Ti-Beta zeotypes with open $Ti(OSi)_3OH$ sites for the efficient epoxidation of cyclohexene with H_2O_2. *J. Catal.* **2024**, *439*, 115748. [CrossRef]
156. Valtchev, V.; Majano, G.; Mintova, S.; Pérez-Ramírez, J. Tailored crystalline microporous materials by post-synthesis modification. *Chem. Soc. Rev.* **2013**, *42*, 263–290. [CrossRef]
157. Lin, H.; Zhang, J.; Duan, Q.; Yang, K.; Liao, W.; Qi, S.; Lü, H.; Zhu, Z. Dealumination-controlled strategy mediates Ti–Y zeolite with cooperative active sites for selective oxidations. *Catal. Sci. Technol.* **2022**, *12*, 4837–4850. [CrossRef]
158. Capel-Sanchez, M.C.; Blanco-Brieva, G.; Campos-Martin, J.M.; de Frutos, M.P.; Wen, W.; Rodriguez, J.A.; Fierro, J.L.G. Grafting strategy to develop single site titanium on an amorphous silica surface. *Langmuir* **2009**, *25*, 7148–7155. [CrossRef] [PubMed]
159. Girelli Consolaro, V.; Rouchon, V.; Baaziz, W.; Hammoumi, A.; Ferté, T.; Pirngruber, G.; Moreaud, M.; Ersen, O. On the properties and origin of mesopore morphologies in dealuminated Faujasite Y zeolites. *Nanoscale* **2025**, *18*, 173–187. [CrossRef]
160. Kononov, P.; Kononova, I.; Moshnikov, V.; Maraeva, E.; Trubetskaya, O. Step-By-Step Modeling and Demetallation Experimental Study on the Porous Structure in Zeolites. *Molecules* **2022**, *27*, 8156. [CrossRef]
161. Pérez-Ramírez, J.; Verboekend, D.; Bonilla, A.; Abelló, S. Zeolite Catalysts with Tunable Hierarchy Factor by Pore-Growth Moderators. *Adv. Funct. Mater.* **2009**, *19*, 3972–3979. [CrossRef]
162. Guisnet, M. "Coke" molecules trapped in the micropores of zeolites as active species in hydrocarbon transformations. *J. Mol. Catal. A Chem.* **2002**, *182–183*, 367–382. [CrossRef]
163. Chen, Z.; Zhang, X.; Yang, F.; Peng, H.; Zhang, X.; Zhu, S.; Che, L. Deactivation of a Y-zeolite based catalyst with coke evolution during the catalytic pyrolysis of polyethylene for fuel oil. *Appl. Catal. A Gen.* **2021**, *609*, 117873. [CrossRef]
164. Horňáček, M.; Horňáčková, M.; Lovás, P.; Veis, P.; Hudec, P.; Smiešková, A.; Velebná, K. The influence of desilication and dealumination on the activity of mordenite catalysts in alkylation of aromatics with 1-alkenes. In Proceedings of the International Zeolite Conference, Moscow, Russia, 7–12 July 2013.
165. Da, Z.; Magnoux, P.; Guisnet, M. Liquid phase alkylation of toluene with 1-heptene over a HFAU zeolite: Evidence for transalkylation between toluene and non-desorbed products. *Appl. Catal. A Gen.* **1999**, *182*, 407–411. [CrossRef]
166. Argyle, M.D.; Bartholomew, C.H. Heterogeneous Catalyst Deactivation and Regeneration: A Review. *Catalysts* **2015**, *5*, 145–269. [CrossRef]
167. Guisnet, M.; Magnoux, P. Organic chemistry of coke formation. *Appl. Catal. A Gen.* **2001**, *212*, 83–96. [CrossRef]
168. Guisnet, M.; Magnoux, P. Deactivation by coking of zeolite catalysts. Prevention of deactivation. Optimal conditions for regeneration. *Catal. Today* **1997**, *36*, 477–483. [CrossRef]
169. Guisnet, M.; Magnoux, P. Coking and deactivation of zeolites: Influence of the Pore Structure. *Appl. Catal.* **1989**, *54*, 1–27. [CrossRef]
170. Guisnet, M.; Costa, L.; Ribeiro, F.R. Prevention of zeolite deactivation by coking. *J. Mol. Catal. A Chem.* **2009**, *305*, 69–83. [CrossRef]
171. Verboekend, D.; Milina, M.; Mitchell, S.; Pérez-Ramírez, J. Hierarchical Zeolites by Desilication: Occurrence and Catalytic Impact of Recrystallization and Restructuring. *Cryst. Growth Des.* **2013**, *13*, 5025–5035. [CrossRef]
172. Zhang, M.; Huang, J.; Meng, F.; Zhang, C.; Zhang, Z. Coke-induced deactivation in zeolite catalysts: Mechanisms, anti-coking modifications, and regeneration approaches. *Dalton Trans.* **2025**, *54*, 17383–17399. [CrossRef] [PubMed]
173. Verboekend, D.; Vilé, G.; Pérez-Ramírez, J. Hierarchical Y and USY Zeolites Designed by Post-Synthetic Strategies. *Adv. Funct. Mater.* **2012**, *22*, 916–928. [CrossRef]
174. McCusker, L.B.; Baerlocher, C. Chapter 3 Zeolite structures. In *Studies in Surface Science and Catalysis*; van Bekkum, H., Flanigen, E.M., Jacobs, P.A., Jansen, J.C., Eds.; Elsevier: Amsterdam, The Netherlands, 2001; Volume 137, pp. 37–67.
175. Rzepka, P.; Sheptyakov, D.; Wang, C.; van Bokhoven, J.A.; Paunović, V. How Micropore Topology Influences the Structure and Location of Coke in Zeolite Catalysts. *ACS Catal.* **2024**, *14*, 5593–5604. [CrossRef]
176. Wen, C.; Lu, L.; Zhang, X.; Jin, K.; Chen, L.; Zhang, Q.; Ma, L.; Wang, C. Optimizing zeolitic hierarchical pore structure to boost the direct conversion of aromatics from syngas over the iron-based/zeolite bifunctional catalysts. *Fuel* **2024**, *357*, 129791. [CrossRef]
177. Horňáček, M.; Hudec, P.; Nociar, A.; Smiešková, A.; Jakubík, T. Activity and regenerability of dealuminated zeolite Y in liquid phase alkylation of benzene with 1-alkene. *Chem. Pap.* **2010**, *64*, 469–474. [CrossRef]
178. Cnudde, P.; Waroquier, M.; Van Speybroeck, V. Universal descriptors for zeolite topology and acidity to predict the stability of butene cracking intermediates. *Catal. Sci. Technol.* **2023**, *13*, 4857–4872. [CrossRef]

179. Soderberg, T. Friedel-Crafts Reactions. Available online: https://chem.libretexts.org/Under_Construction/Purgatory/Book:_Organic_Chemistry_with_a_Biological_Emphasis_(Soderberg)/15:_Electrophilic_reactions/15.06:_Synthetic_parallel_-_electrophilic_aromatic_substitution_in_the_lab (accessed on 29 November 2025).
180. Deshlahra, P.; Iglesia, E. Reactivity descriptors in acid catalysis: Acid strength, proton affinity and host–guest interactions. *Chem. Commun.* **2020**, *56*, 7371–7398. [CrossRef] [PubMed]
181. Craciun, I.; Reyniers, M.-F.; Marin, G.B. Liquid-phase alkylation of benzene with octenes over Y zeolites: Kinetic modeling including acidity descriptors. *J. Catal.* **2012**, *294*, 136–150. [CrossRef]
182. Zhang, J.; Zhu, Z.; Li, C.; Wen, L.; Min, E. Characterization and kinetic investigation of tungstophosphoric supported on SiO2 for alkylation of benzene with 1-dodecene to synthesize linear alkylbenzene. *J. Mol. Catal. A Chem.* **2003**, *198*, 359–367. [CrossRef]
183. Kirumakki, S.R.; Nagaraju, N.; Narayanan, S. A comparative esterification of benzyl alcohol with acetic acid over zeolites Hβ, HY and HZSM5. *Appl. Catal. A Gen.* **2004**, *273*, 1–9. [CrossRef]
184. Bocus, M.; Vanduyfhuys, L.; De Proft, F.; Weckhuysen, B.M.; Van Speybroeck, V. Mechanistic Characterization of Zeolite-Catalyzed Aromatic Electrophilic Substitution at Realistic Operating Conditions. *JACS Au* **2022**, *2*, 502–514. [CrossRef]
185. Ji, Y.; Liu, Z.; Zhao, Z.; Gao, P.; Bao, X.; Chen, K.; Hou, G. Untangling Framework Confinements: A Dynamical Study on Bulky Aromatic Molecules in MFI Zeolites. *ACS Catal.* **2022**, *12*, 15288–15297. [CrossRef]
186. Gong, X.; Çağlayan, M.; Ye, Y.; Liu, K.; Gascon, J.; Dutta Chowdhury, A. First-Generation Organic Reaction Intermediates in Zeolite Chemistry and Catalysis. *Chem. Rev.* **2022**, *122*, 14275–14345. [CrossRef]
187. He, M.; Qie, G.; Ali, M.F.; Rizwan, M.; Song, Y.; Zhou, X. Study of Coke Formation Mechanism on HZSM-5 Zeolite During Co-cracking of n-Hexane and Alcohols. *Catal. Lett.* **2024**, *154*, 3628–3644. [CrossRef]
188. Da, Z.; Magnoux, P.; Guisnet, M. Alkylation of toluene with 1-dodecene over HFAU zeolite. Deactivation and regeneration. *Catal. Lett.* **1999**, *61*, 203–206. [CrossRef]
189. Sui, H.; Chen, Y.; Chen, H.; Zhao, Y.; Tian, C.; Chen, W.; Chang, C.; Pang, S.; Li, P. Characterization and mechanistic insights into coke formation on biochar-based catalysts under microwave-assisted biomass pyrolysis. *Ind. Crops Prod.* **2025**, *226*, 120645. [CrossRef]
190. Weitkamp, J. Zeolites and catalysis. *Solid State Ion.* **2000**, *131*, 175–188. [CrossRef]
191. Bauer, F.; Karge, H.G. Characterization of Coke on Zeolites. In *Characterization II*; Karge, H.G., Weitkamp, J., Eds.; Springer: Berlin/Heidelberg, Germany, 2007; pp. 249–364.
192. Quintana-Gómez, L.; Connolly, M.; Shehab, A.K.; Al-Shathr, A.; McGregor, J. "Reverse combustion" of carbon dioxide in water: The influence of reaction conditions. *Front. Energy Res.* **2022**, *10*, 917943. [CrossRef]
193. Bartholomew, C.H. Mechanisms of catalyst deactivation. *Appl. Catal. A Gen.* **2001**, *212*, 17–60. [CrossRef]
194. Zwain, A.; Shakor, Z.; Al-Zaidi, B. An active Ni/Kaolin-Bentonite double-bed catalyst for hydrodesulfurization of Iraqi gas oil. *AIP Conf. Proc.* **2025**, *3350*, 040001. [CrossRef]
195. Zheng, H.; Xu, R.; Zhang, J.; Daghagheleh, O.; Schenk, J.; Li, C.; Wang, W. A Comprehensive Review of Characterization Methods for Metallurgical Coke Structures. *Materials* **2022**, *15*, 174. [CrossRef] [PubMed]
196. Liu, B.; Slocombe, D.; AlKinany, M.; AlMegren, H.; Wang, J.; Arden, J.; Vai, A.; Gonzalez-Cortes, S.; Xiao, T.; Kuznetsov, V.; et al. Advances in the study of coke formation over zeolite catalysts in the methanol-to-hydrocarbon process. *Appl. Petrochem. Res.* **2016**, *6*, 209–215. [CrossRef]
197. Anekwe, I.M.S.; Isa, Y.M. Unlocking catalytic longevity: A critical review of catalyst deactivation pathways and regeneration technologies. *Energy Adv.* **2025**, *4*, 1075–1113. [CrossRef]
198. Agra, A.A.; Nicolodi, A.; Flores, B.D.; Flores, I.V.; da Silva, G.L.R.; Vilela, A.C.F.; Osório, E. Automated procedure for coke microstructural characterization in imagej software aiming industrial application. *Fuel* **2021**, *304*, 121374. [CrossRef]
199. Zhang, C.C.; Hartlaub, S.; Petrovic, I.; Yilmaz, B. Raman Spectroscopy Characterization of Amorphous Coke Generated in Industrial Processes. *ACS Omega* **2022**, *7*, 2565–2570. [CrossRef] [PubMed]
200. Suwardiyanto; Howe, R.F.; Gibson, E.K.; Catlow, C.R.A.; Hameed, A.; McGregor, J.; Collier, P.; Parker, S.F.; Lennon, D. An assessment of hydrocarbon species in the methanol-to-hydrocarbon reaction over a ZSM-5 catalyst. *Faraday Discuss.* **2017**, *197*, 447–471. [CrossRef] [PubMed]
201. Gomez, L.Q.; Shehab, A.K.; Al-Shathr, A.; Ingram, W.; Konstantinova, M.; Cumming, D.; McGregor, J. H2-free Synthesis of Aromatic, Cyclic and Linear Oxygenates from CO2. *ChemSusChem* **2020**, *13*, 647–658. [CrossRef] [PubMed]
202. Sørensen, M.D.P. The establishment of a coke-burn kinetic model for zeolite catalysts. *Chem. Eng. Sci.* **2017**, *168*, 465–479. [CrossRef]
203. Wang, T.; Chen, M.; Liu, X.; Zhang, Z.-G.; Xu, Y. Distinguishing external and internal coke depositions on micron-sized HZSM-5 via catalyst-assisted temperature-programmed oxidation. *New J. Chem.* **2019**, *43*, 13938–13946. [CrossRef]
204. Grey, C.P.; Dupré, N. NMR Studies of Cathode Materials for Lithium-Ion Rechargeable Batteries. *Chem. Rev.* **2004**, *104*, 4493–4512. [CrossRef]

205. Quoineaud, A.A.; Montouillout, V.; Gautier, S.; Lacombe, S.; Fernandez, C. Characterization and quantification of aluminum species in zeolites using high-resolution 27Al solid state NMR. In *Studies in Surface Science and Catalysis*; Aiello, R., Giordano, G., Testa, F., Eds.; Elsevier: Amsterdam, The Netherlands, 2002; Volume 142, pp. 391–397.
206. Loppnow, G.R.; Shoute, L.; Schmidt, K.J.; Savage, A.; Hall, R.H.; Bulmer, J.T. UV Raman spectroscopy of hydrocarbons. *Philos. Trans. Ser. A Math. Phys. Eng. Sci.* **2004**, *362*, 2461–2476. [CrossRef]
207. Wennmacher, J.T.C.; Mahmoudi, S.; Rzepka, P.; Sik Lee, S.; Gruene, T.; Paunović, V.; van Bokhoven, J.A. Electron Diffraction Enables the Mapping of Coke in ZSM-5 Micropores Formed during Methanol-to-Hydrocarbons Conversion. *Angew. Chem. Int. Ed. Engl.* **2022**, *61*, e202205413. [CrossRef]
208. Nejadmoghadam, E.; Achour, A.; Öhrman, O.; Creaser, D.; Olsson, L. Understanding catalyst deactivation in an industrial green hydrotreater and its correlation with catalyst composition. *Fuel Process. Technol.* **2025**, *276*, 108260. [CrossRef]
209. Chen, Z.; Zhang, L.; Yu, Y.; Liu, D.; Fang, N.; Liu, Y.; He, M. Molecular traffic control for catalytic oxidation reaction in TS-1 zeolite. *Microporous Mesoporous Mater.* **2022**, *332*, 111715. [CrossRef]
210. Zhou, L.; Zhao, H.; Tong, Y.; Gao, J.; Hao, X.; Yang, Y.; Li, Y. Evolution of Coke Formation and Its Effect on β-Zeolite in Catalytic Cracking. *Ind. Eng. Chem. Res.* **2022**, *61*, 17440–17456. [CrossRef]
211. Liu, Y.; Zhang, X.; Wang, Z.; Li, J.; Lv, Q.; Wang, D.; Zhao, S.; Wang, L.; Zhang, S.; Pan, Y. Zeolite-Anchored Single-Atom Catalysts for Enhanced Hydrogenation and Dehydrogenation Reaction Process. *Adv. Mater.* **2026**, *38*, e13175. [CrossRef]
212. Hita, I.; Mohamed, H.O.; Attada, Y.; Zambrano, N.; Zhang, W.; Ramírez, A.; Castaño, P. Direct analysis at temporal and molecular level of deactivating coke species formed on zeolite catalysts with diverse pore topologies. *Catal. Sci. Technol.* **2023**, *13*, 1288–1300. [CrossRef]
213. Bienz, S.; van Vreeswijk, S.H.; Pandey, Y.; Bartolomeo, G.L.; Weckhuysen, B.M.; Zenobi, R.; Kumar, N. Probing coke formation during the methanol-to-hydrocarbon reaction on zeolite ZSM-5 catalyst at the nanoscale using tip-enhanced fluorescence microscopy. *Catal. Sci. Technol.* **2022**, *12*, 5795–5801. [CrossRef] [PubMed]
214. Abdulkareem-Alsultan, G.; Asikin-Mijan, N.; Obeas, L.K.; Yunus, R.; Razali, S.Z.; Islam, A.; Hin Taufiq-Yap, Y. In-situ operando and ex-situ study on light hydrocarbon-like-diesel and catalyst deactivation kinetic and mechanism study during deoxygenation of sludge oil. *Chem. Eng. J.* **2022**, *429*, 132206. [CrossRef]
215. Cordero-Lanzac, T.; Bilbao, J. Deactivation kinetic models for the fluid catalytic cracking (FCC). A review. *Chem. Eng. J.* **2025**, *514*, 162856. [CrossRef]
216. Zhou, J.; Zhao, J.; Zhang, J.; Zhang, T.; Ye, M.; Liu, Z. Regeneration of catalysts deactivated by coke deposition: A review. *Chin. J. Catal.* **2020**, *41*, 1048–1061. [CrossRef]
217. Bao, R.; Lei, C.; Wang, C.; Zhou, F. Thermal Reaction Process and Thermokinetic Characteristics of Coking Coal Oxidation. *Fire* **2024**, *7*, 448. [CrossRef]
218. Safarzadeh Kozani, P.; Safarzadeh Kozani, P.; Hamidi, M.; Valentine Okoro, O.; Eskandani, M.; Jaymand, M. Polysaccharide-based hydrogels: Properties, advantages, challenges, and optimization methods for applications in regenerative medicine. *Int. J. Polym. Mater. Polym. Biomater.* **2022**, *71*, 1319–1333. [CrossRef]
219. Ellison, C.; Hoffman, J.; Shekhawat, D. Comparison of microwave and conventional heating for CO_2 desorption from zeolite 13X. *Int. J. Greenh. Gas Control* **2021**, *107*, 103311. [CrossRef]
220. Amornsin, P.O.; Nokpho, P.; Wang, X.; Piumsomboon, P.; Chalermsinsuwan, B. Investigation of microwave-assisted regeneration of zeolite 13X for efficient direct air CO_2 capture: A comparison with conventional heating method. *Sci. Rep.* **2025**, *15*, 18376. [CrossRef]
221. Shan, N.; Zhou, M.; Hanchett, M.K.; Chen, J.; Liu, B. Practical principles of density functional theory for catalytic reaction simulations on metal surfaces—From theory to applications. *Mol. Simul.* **2017**, *43*, 861–885. [CrossRef]
222. Semnani, P.; Bogojeski, M.; Bley, F.; Zhang, Z.; Wu, Q.; Kneib, T.; Herrmann, J.; Weisser, C.; Patcas, F.; Müller, K.-R. A Machine Learning and Explainable AI Framework Tailored for Unbalanced Experimental Catalyst Discovery. *J. Phys. Chem. C* **2024**, *128*, 21349–21367. [CrossRef]
223. Costa, C.S.; Ribeiro, M.R.; Silva, J.M. Catalyst Accessibility and Acidity in the Hydrocracking of HDPE: A Comparative Study of H-USY, H-ZSM-5, and MCM-41 Modified with Ga and Al. *Molecules* **2024**, *29*, 4248. [CrossRef]
224. Tanabe, K.; Hölderich, W.F. Industrial application of solid acid–base catalysts. *Appl. Catal. A Gen.* **1999**, *181*, 399–434. [CrossRef]
225. Mériaudeau, P.; Ben Taarit, Y.; Thangaraj, A.; Almeida, J.L.G.; Naccache, C. Zeolite based catalysts for linear alkylbenzene production: Dehydrogenation of long chain alkanes and benzene alkylation. *Catal. Today* **1997**, *38*, 243–247. [CrossRef]
226. Kuai, L.; Wang, M.; Meng, X.; Shi, L.; Liu, N. W Modified HY Zeolite as Catalyst for Alkylation of Aromatic. *Catal. Lett.* **2022**, *152*, 2480–2490. [CrossRef]
227. Fattahi, N.; Triantafyllidis, K.; Luque, R.; Ramazani, A. Zeolite-Based Catalysts: A Valuable Approach toward Ester Bond Formation. *Catalysts* **2019**, *9*, 758. [CrossRef]
228. Cowley, M.; de Klerk, A.; Nel, R.J.J. Amylation of Toluene by Solid Acid Catalysis. *Ind. Eng. Chem. Res.* **2005**, *44*, 5535–5541. [CrossRef]

229. Yuan, X.-D.; Park, J.-N.; Wang, J.; Lee, C.; Park, S.-E. Alkylation of benzene with 1- dodecene over usy zeolite catalyst: Effect of pretreatment and reaction conditions. *Korean J. Chem. Eng.* **2002**, *19*, 607–610. [CrossRef]
230. Hussain, H. Aromatic Disproportionation and Transalkylation over Modified Beta Zeolites. Ph.D. Thesis, University of Manchester, Manchester, UK, 2023.
231. Weitkamp, J.; Puppe, L. *Catalysis and Zeolites*; Springer: New York, NY, USA, 1999.
232. Qian, K.; Tian, W.; Yang, Z.; Xu, J.; Pan, H.; Yin, L.; Chen, D. Unraveling the Role of Mesoporosity and Acidity of Hierarchical Aggregated HZSM-5 in HDPE Vapor Catalytic Cracking for Value-Added Hydrocarbons. *Ind. Eng. Chem. Res.* **2024**, *63*, 16324–16334. [CrossRef]
233. Liu, M.; Miao, C.; Wu, Z. Recent advances in the synthesis, characterization, and catalytic consequence of metal species confined within zeolite for hydrogen-related reactions. *Ind. Chem. Mater.* **2024**, *2*, 57–84. [CrossRef]
234. Tang, B.; Dai, W.; Sun, X.; Wu, G.; Li, L.; Guan, N.; Hunger, M. Incorporation of cerium atoms into Al-free Beta zeolite framework for catalytic application. *Chin. J. Catal.* **2015**, *36*, 801–805. [CrossRef]
235. Khalil, M.; Al-Zaidi, B.Y.; Shakor, Z.M.; Hussein, S.J.; Al-Shathr, A. Experimental and Kinetic Study of the Catalytic Behavior of Sulfate-Treated Nanostructured Bifunctional Zirconium Oxide Catalysts in n-Heptane Hydroisomerization Reactions. *Chemengineering* **2023**, *7*, 115. [CrossRef]
236. Hu, Z.-P.; Qin, G.; Han, J.; Zheng, Y.; Liu, Z.; Jiang, Y.; Su, X.; Ji, T.; Li, M.; Yuan, Z.-Y.; et al. Synergy principle of single active centers and microenvironment for Cr-MFI-catalyzed alkane dehydrogenation. *Natl. Sci. Rev.* **2025**, *12*, nwaf405. [CrossRef] [PubMed]
237. Al-Shathr, A.; Shakor, Z.M.; Majdi, H.S.; AbdulRazak, A.A.; Albayati, T.M. Comparison between Artificial Neural Network and Rigorous Mathematical Model in Simulation of Industrial Heavy Naphtha Reforming Process. *Catalysts* **2021**, *11*, 1034. [CrossRef]

Disclaimer/Publisher's Note: The statements, opinions and data contained in all publications are solely those of the individual author(s) and contributor(s) and not of MDPI and/or the editor(s). MDPI and/or the editor(s) disclaim responsibility for any injury to people or property resulting from any ideas, methods, instructions or products referred to in the content.